FIR Filter Approximations

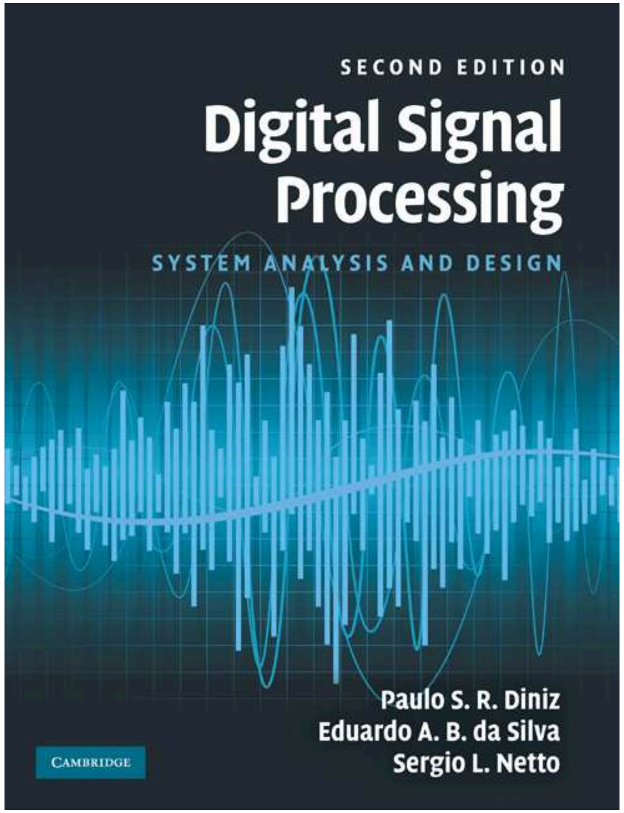

Paulo S. R. Diniz

Eduardo A. B. da Silva

Sergio L. Netto

diniz,eduardo,sergioln@lps.ufrj.br

September 2010

Contents

Contents (cont.)

Introduction

- In this chapter, we will study the approximation schemes for digital filters with finite-duration impulse response (FIR) and we will present the methods for determining the multiplier coefficients and the filter order, in such a way that the resulting frequency response satisfies a set of prescribed specifications.
- In some cases, FIR filters are considered inefficient in the sense that they require a high-order transfer function to satisfy the system requirements when compared to the order required by digital filters with infinite-duration impulse response.
- However, FIR digital filters do possess a few implementation advantages such as a possible exact linear-phase characteristic and intrinsically stable implementations, when using non-recursive realizations. In addition, the computational complexity of FIR digital filters can be reduced if they are implemented using fast numerical algorithms such as the fast Fourier transform.

Introduction

- We start by discussing the ideal frequency response characteristics of commonly used FIR filters, as well as their corresponding impulse responses. We include in the discussion lowpass, highpass, bandpass, and bandstop filters, and also treat two other important filters, namely differentiators and Hilbert transformers.
- We go on to discuss the frequency sampling and the window methods for approximating FIR digital filters, focusing on the rectangular, triangular, Bartlett, Hamming, Blackman, Kaiser, and Dolph-Chebyshev windows. In addition, the design of maximally flat FIR filters is addressed.

Introduction

- Following this, numerical methods for designing FIR filters are discussed. A unified framework for the general approximation problem is provided. The weighted-least-squares (WLS) method is presented as a generalization of the rectangular window approach. We then introduce the Chebyshev (or minimax) approach as the most efficient form, with respect to the resulting filter order, to approximate FIR filters which minimize the maximum passband and stopband ripples. We also discuss the WLS-Chebyshev approach, which is able to combine the desired characteristics of high attenuation of the Chebyshev scheme with the low energy level of the WLS scheme in the filter stopband.

- We conclude the chapter by discussing the use of MATLAB for designing FIR filters.

Ideal characteristics of standard filters

- In this section, we analyze the time and frequency response characteristics of commonly used FIR filters. First, we deal with lowpass, highpass, bandpass, and bandstop filters. Then, two types of filters widely used in the field of digital signal processing, the differentiators and Hilbert transformers, are analyzed, and their implementations as special cases of FIR digital filters are studied.

- The behavior of a filter is usually best characterized by its frequency response $H(e^{j\omega})$. As seen in Chapter 4, a filter implementation is based on its transfer function $H(z)$ of the form

$$H(z) = \sum_{n=-\infty}^{\infty} h(n) z^{-n} \tag{1}$$

- The FIR filter design starts by calculating the coefficients $h(n)$ which will be used in one of the structures discussed in Section 4.2.

Ideal characteristics of standard filters

- As seen in Section 2.8, the relationship between $H(e^{j\omega})$ and $h(n)$ is given by the following pair of equations:

$$H(e^{j\omega}) = \sum_{n=-\infty}^{\infty} h(n)e^{-j\omega n} \tag{2}$$

$$h(n) = \frac{1}{2\pi}\int_{-\pi}^{\pi} H(e^{j\omega})e^{j\omega n}d\omega \tag{3}$$

- In what follows, we determine $H(e^{j\omega})$ and $h(n)$ related to ideal standard filters.

Lowpass, highpass, bandpass, and bandstop filters

- The ideal magnitude responses of some standard digital filters are depicted below.

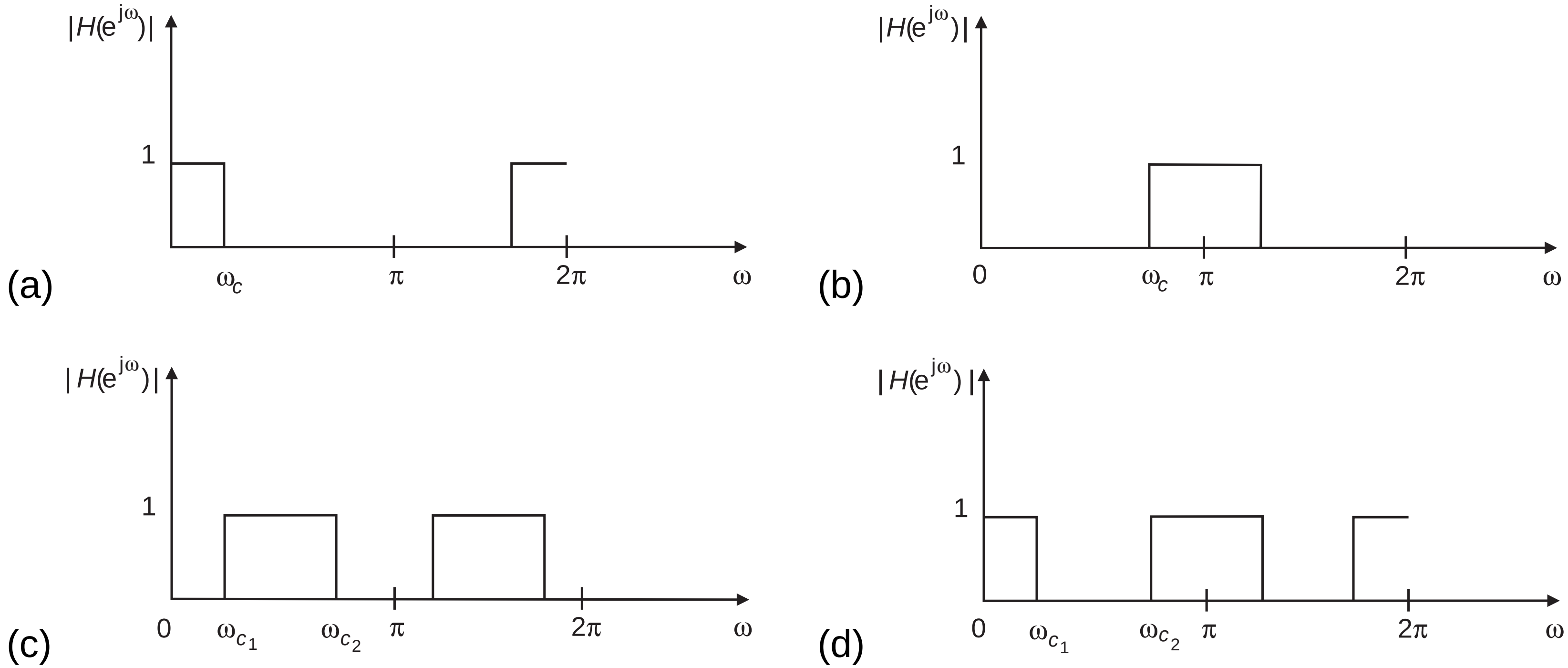

Figure 1: Ideal magnitude responses: (a) lowpass; (b) highpass; (c) bandpass; (d) bandstop filters.

Lowpass, highpass, bandpass, and bandstop filters

- For instance, the lowpass filter, as seen in Figure 1a, is described by

$$|H(e^{j\omega})| = \begin{cases} 1, & \text{for } |\omega| \leq \omega_c \\ 0, & \text{for } \omega_c < |\omega| \leq \pi \end{cases} \tag{4}$$

- Using (3), the impulse response for the ideal lowpass filter is

$$h(n) = \frac{1}{2\pi}\int_{-\omega_c}^{\omega_c} e^{j\omega n} d\omega = \begin{cases} \dfrac{\omega_c}{\pi}, & \text{for } n = 0 \\ \dfrac{\sin(\omega_c n)}{\pi n}, & \text{for } n \neq 0 \end{cases} \tag{5}$$

- One should note that in the above inverse transform calculations we have supposed that the phase of the filter is zero.

Lowpass, highpass, bandpass, and bandstop filters

- From Section 4.2.3, we have that the phase of an FIR filter must be of the form $e^{-j\omega\frac{M}{2}}$, where M is an integer.
- Therefore, for M even, it suffices to shift the above impulse response by $\frac{M}{2}$ samples. However, for M odd, $\frac{M}{2}$ is not an integer, and the impulse response must be computed as

$$
\begin{aligned}
h(n) &= \frac{1}{2\pi}\int_{-\omega_c}^{\omega_c} e^{-j\omega\frac{M}{2}} e^{j\omega n} d\omega \\
&= \frac{1}{2\pi}\int_{-\omega_c}^{\omega_c} e^{j\omega\left(n-\frac{M}{2}\right)} d\omega \\
&= \frac{\sin\left[\omega_c\left(n-\frac{M}{2}\right)\right]}{\pi\left(n-\frac{M}{2}\right)}
\end{aligned}
\tag{6}
$$

Lowpass, highpass, bandpass, and bandstop filters

- Likewise, for bandstop filters, the ideal magnitude response, depicted in Figure 1d, is given by

$$|H(e^{j\omega})| = \begin{cases} 1, & \text{for} \quad 0 \leq |\omega| \leq \omega_{c_1} \\ 0, & \text{for} \quad \omega_{c_1} < |\omega| < \omega_{c_2} \\ 1, & \text{for} \quad \omega_{c_2} \leq |\omega| \leq \pi \end{cases} \tag{7}$$

- Then, using (3), the impulse response for such an ideal filter is

$$\begin{aligned} h(n) &= \frac{1}{2\pi}\left[\int_{-\omega_{c_1}}^{\omega_{c_1}} e^{j\omega n} d\omega + \int_{\omega_{c_2}}^{\pi} e^{j\omega n} d\omega + \int_{-\pi}^{-\omega_{c_2}} e^{j\omega n} d\omega\right] \\ &= \begin{cases} 1 + \dfrac{\omega_{c_1} - \omega_{c_2}}{\pi}, & \text{for } n = 0 \\ \dfrac{1}{\pi n}\left[\sin(\omega_{c_1} n) - \sin(\omega_{c_2} n)\right], & \text{for } n \neq 0 \end{cases} \end{aligned} \tag{8}$$

Lowpass, highpass, bandpass, and bandstop filters

- Again, the above impulse response is valid only for zero phase. For non-zero linear phase, the discussion following equation (5) applies.
- Following an analogous reasoning, one can easily find the magnitude responses of the ideal highpass and bandpass filters, depicted in Figures 1b and 1c, respectively.
- Table 1 (Subsection 5.2.4) includes the ideal magnitude responses and their respective impulse responses for the ideal zero-phase lowpass, highpass, bandpass, and bandstop filters. The nonzero-phase case is considered in Exercise 5.1.

Differentiators

- An ideal discrete-time differentiator is a linear system that, when samples of a band-limited continuous signal are used as input, the output samples represent the derivative of the continuous signal.

- More precisely, given a continuous-time signal $x_a(t)$ band-limited to $\left[-\frac{\pi}{T}, \frac{\pi}{T}\right)$, when its corresponding sampled version $x(n) = x_a(nT)$ is input to an ideal differentiator, it produces the output signal, $y(n)$, such that

$$y(n) = \left.\frac{dx_a(t)}{dt}\right|_{t=nT} \tag{9}$$

- If the Fourier transform of the continuous-time signal is denoted by $X_a(j\Omega)$, we have that the Fourier transform of its derivative is $j\Omega X_a(j\Omega)$.

Differentiators

- Therefore, an ideal discrete-time differentiator is characterized by a frequency response, up to a multiplicative constant, of the form

$$H(e^{j\omega}) = j\omega, \text{ for } -\pi \leq \omega < \pi \tag{10}$$

- The magnitude and phase responses of a differentiator are depicted in Figure 2.

Differentiators

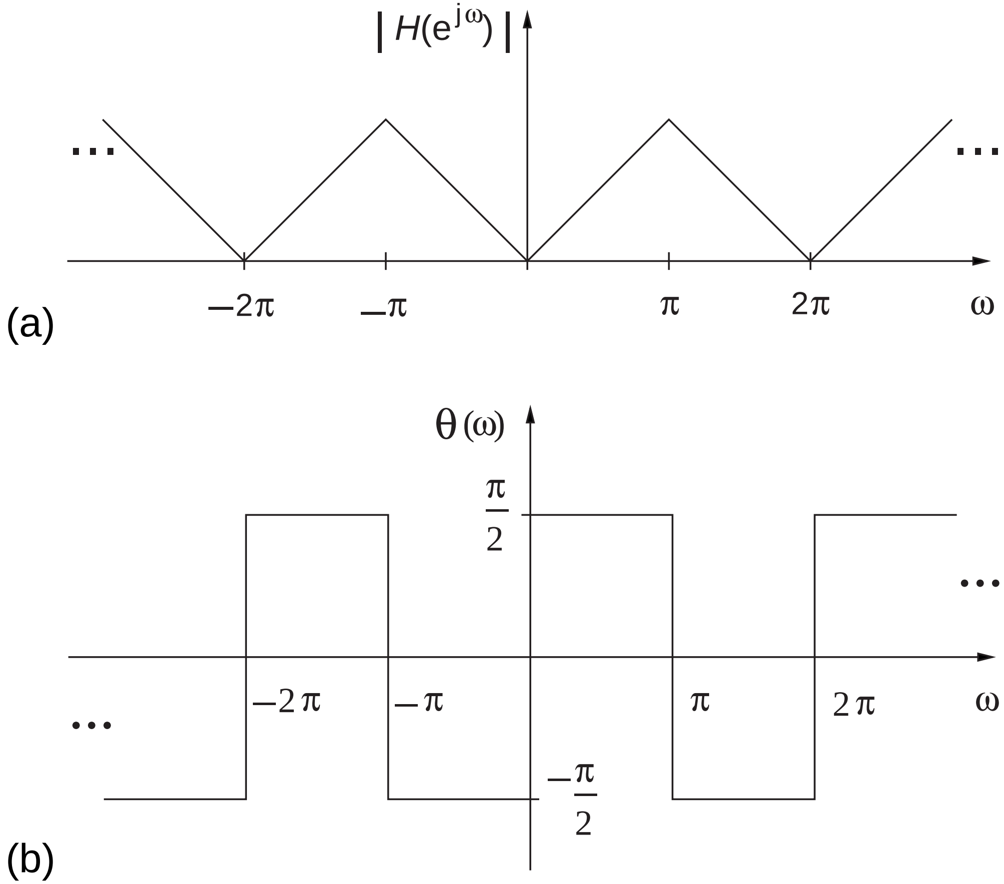

Figure 2: Characteristics of an ideal discrete-time differentiator: (a) magnitude response; (b) phase response.

Differentiators

- Using equation (3), the corresponding impulse response is given by

$$
\begin{aligned}
h(n) &= \frac{1}{2\pi}\int_{-\pi}^{\pi} j\omega e^{j\omega n} d\omega \\
&= \begin{cases} 0, & \text{for } n = 0 \\ \frac{1}{2\pi}\left[e^{j\omega n}\left(\frac{\omega}{n} - \frac{1}{jn^2}\right)\right]\Big|_{-\pi}^{\pi} = \frac{(-1)^n}{n}, & \text{for } n \neq 0 \end{cases}
\end{aligned}
\tag{11}
$$

- One should note that if a differentiator is to be approximated by a linear-phase FIR filter, one should necessarily use either a Type-III or a Type-IV form.

Differentiators

- In fact, using an argument similar to the one following equation (5), we can see that the above equation can be used only in the case of Type-III filters. For Type-IV filters, we must perform a derivation similar to the one in equation (6).

Hilbert transformers

- The Hilbert transformer is a system that, when fed with the real part of a complex signal whose Fourier transform is null for $-\pi \leq \omega < 0$, produces at its output the imaginary part of the complex signal.

- In other words, let $x(n)$ be the inverse Fourier transform of $X(e^{j\omega})$ such that $X(e^{j\omega}) = 0$, $-\pi \leq \omega < 0$. The real and imaginary parts of $x(n)$, $x_R(n)$ and $x_I(n)$, are defined as

$$\left.\begin{aligned} \mathrm{Re}\{x(n)\} &= \frac{x(n) + x^*(n)}{2} \\ \mathrm{Im}\{x(n)\} &= \frac{x(n) - x^*(n)}{2j} \end{aligned}\right\} \tag{12}$$

Hilbert transformers

- Hence, their Fourier transforms, $X_R(e^{j\omega}) = \mathcal{F}\{\text{Re}\{x(n)\}\}$ and $X_I(e^{j\omega}) = \mathcal{F}\{\text{Im}\{x(n)\}\}$, are

$$\left.\begin{aligned} X_R(e^{j\omega}) &= \frac{X(e^{j\omega}) + X^*(e^{-j\omega})}{2} \\ X_I(e^{j\omega}) &= \frac{X(e^{j\omega}) - X^*(e^{-j\omega})}{2j} \end{aligned}\right\} \tag{13}$$

- For $-\pi \leq \omega < 0$, since $X(e^{j\omega}) = 0$, we have that

$$\left.\begin{aligned} X_R(e^{j\omega}) &= \frac{X^*(e^{-j\omega})}{2} \\ X_I(e^{j\omega}) &= j\frac{X^*(e^{-j\omega})}{2} \end{aligned}\right\} \tag{14}$$

Hilbert transformers

- And, for $0 \leq \omega < \pi$, since $X^*(e^{-j\omega}) = 0$, we also have that

$$\left.\begin{aligned} X_R(e^{j\omega}) &= \frac{X(e^{j\omega})}{2} \\ X_I(e^{j\omega}) &= -j\frac{X(e^{j\omega})}{2} \end{aligned}\right\} \tag{15}$$

- From equations (14) and (15), we can easily conclude that

$$\left.\begin{aligned} X_I(e^{j\omega}) &= -jX_R(e^{j\omega}), \quad \text{for } 0 \leq \omega < \pi \\ X_I(e^{j\omega}) &= jX_R(e^{j\omega}), \quad \text{for } -\pi \leq \omega < 0 \end{aligned}\right\} \tag{16}$$

Hilbert transformers

- These equations provide a relation between the Fourier transforms of the real and imaginary parts of a signal whose Fourier transform is null for $-\pi \leq \omega < 0$. It thus implies that the ideal Hilbert transformer has the following transfer function:

$$H(e^{j\omega}) = \begin{cases} -j, & \text{for } 0 \leq \omega < \pi \\ j, & \text{for } -\pi \leq \omega < 0 \end{cases} \tag{17}$$

- The magnitude and phase components of such a frequency response are depicted in Figure 3.

Hilbert transformers

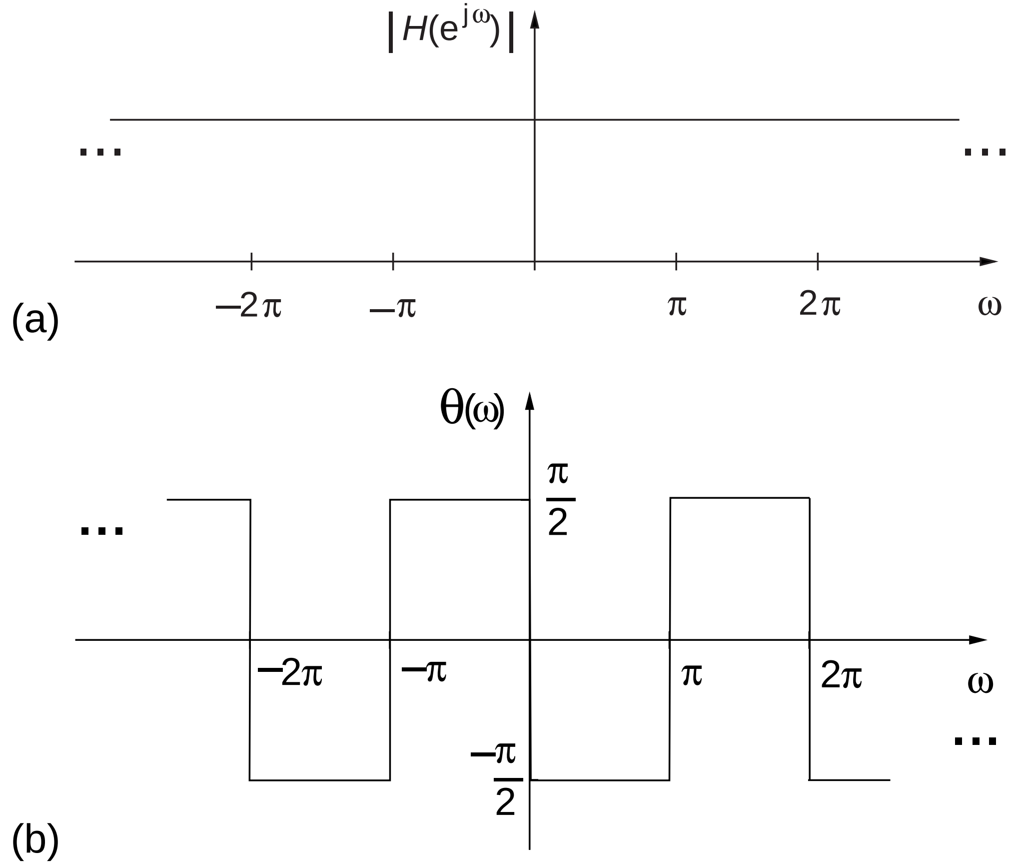

Figure 3: Characteristics of an ideal Hilbert transformer: (a) magnitude response; (b) phase response.

Hilbert transformers

- Using equation (3), the corresponding impulse response for the ideal Hilbert transformer is given by

$$h(n) = \frac{1}{2\pi}\left[\int_{0}^{\pi} -\mathrm{j}e^{\mathrm{j}\omega n} d\omega + \int_{-\pi}^{0} \mathrm{j}e^{\mathrm{j}\omega n} d\omega\right] = \begin{cases} 0, & \text{for } n = 0 \\ \frac{1}{\pi n}\left[1-(-1)^{n}\right], & \text{for } n \neq 0 \end{cases} \tag{18}$$

- By examining equation (17) we conclude, as in the case of the differentiator, that a Hilbert transformer must be approximated, when using a linear-phase FIR filter, by either a Type-III or Type-IV structure.

Hilbert transformers

- An interesting interpretation of Hilbert transformers comes from the observation that equation (17) implies that every positive-frequency sinusoid $e^{j\omega_0}$ input to a Hilbert transformer has its phase shifted by $-\frac{\pi}{2}$ at the output, whereas every negative-frequency sinusoid $e^{-j\omega_0}$ has its phase shifted by $+\frac{\pi}{2}$ at the output, as seen in Figure 3b.

- This is equivalent to shifting the phase of every sine or cosine function by $-\frac{\pi}{2}$. Therefore, an ideal Hilbert transformer transforms every "cosine" component of a signal into a "sine" and every "sine" component into a "cosine".

Summary

- Table 1 summarizes the ideal frequency responses and corresponding impulse responses for the basic lowpass, highpass, bandpass, and bandstop filters, as well as for differentiators and Hilbert transformers.

- By examining this table, we note that the impulse responses corresponding to all these ideal filters are not directly realizable, since they have infinite duration and are noncausal. In the remainder of this chapter, we deal with the problem of approximating ideal frequency responses, as the ones seen in this section, by a digital filter with a finite-duration impulse response.

Summary

Table 1: Ideal frequency characteristics and corresponding impulse responses for lowpass, highpass, bandpass, and bandstop filters, as well as for differentiators and Hilbert transformers.

Filter type	Magnitude response $\lvert H(e^{j\omega})\rvert$	Impulse response $h(n)$
Lowpass	$\begin{cases} 1, & \text{for } 0 \leq \lvert\omega\rvert \leq \omega_c \\ 0, & \text{for } \omega_c < \lvert\omega\rvert \leq \pi \end{cases}$	$\begin{cases} \dfrac{\omega_c}{\pi}, & \text{for } n = 0 \\ \dfrac{1}{\pi n}\sin(\omega_c n), & \text{for } n \neq 0 \end{cases}$
Highpass	$\begin{cases} 0, & \text{for } 0 \leq \lvert\omega\rvert < \omega_c \\ 1, & \text{for } \omega_c \leq \lvert\omega\rvert \leq \pi \end{cases}$	$\begin{cases} 1 - \dfrac{\omega_c}{\pi}, & \text{for } n = 0 \\ -\dfrac{1}{\pi n}\sin(\omega_c n), & \text{for } n \neq 0 \end{cases}$

Summary

Filter type	Magnitude response $\lvert H(e^{j\omega})\rvert$	Impulse response $h(n)$
Bandpass	$\begin{cases} 0, & \text{for } 0 \le \lvert\omega\rvert < \omega_{c_1} \\ 1, & \text{for } \omega_{c_1} \le \lvert\omega\rvert \le \omega_{c_2} \\ 0, & \text{for } \omega_{c_2} < \lvert\omega\rvert \le \pi \end{cases}$	$\begin{cases} \dfrac{(\omega_{c_2} - \omega_{c_1})}{\pi}, & \text{for } n = 0 \\ \dfrac{1}{\pi n}\left[\sin(\omega_{c_2} n) - \sin(\omega_{c_1} n)\right], & \text{for } n \neq 0 \end{cases}$
Bandstop	$\begin{cases} 1, & \text{for } 0 \le \lvert\omega\rvert \le \omega_{c_1} \\ 0, & \text{for } \omega_{c_1} < \lvert\omega\rvert < \omega_{c_2} \\ 1, & \text{for } \omega_{c_2} \le \lvert\omega\rvert \le \pi \end{cases}$	$\begin{cases} 1 - \dfrac{(\omega_{c_2} - \omega_{c_1})}{\pi}, & \text{for } n = 0 \\ \dfrac{1}{\pi n}\left[\sin(\omega_{c_1} n) - \sin(\omega_{c_2} n)\right], & \text{for } n \neq 0 \end{cases}$

Summary

Filter type	Frequency response $H(e^{j\omega})$	Impulse response $h(n)$
Differentiator	$j\omega, \quad \text{for } -\pi \leq \omega < \pi$	$\begin{cases} 0, & \text{for } n = 0 \\ \dfrac{(-1)^n}{n}, & \text{for } n \neq 0 \end{cases}$
Hilbert transformer	$\begin{cases} -j, & \text{for } 0 \leq \omega < \pi \\ j, & \text{for } -\pi \leq \omega < 0 \end{cases}$	$\begin{cases} 0, & \text{for } n = 0 \\ \dfrac{1}{\pi n}\left[1 - (-1)^n\right], & \text{for } n \neq 0 \end{cases}$

FIR filter approximation by frequency sampling

- In general, the problem of FIR filter design is to find a finite-length impulse response $h(n)$, whose Fourier transform $H(e^{j\omega})$ approximates a given frequency response well enough.

- As seen in Section 3.2, one way of achieving such a goal is by noting that the DFT of a length-N sequence $h(n)$ corresponds to samples of its Fourier transform at the frequencies $\omega = \frac{2\pi k}{N}$, that is

$$H(e^{j\omega}) = \sum_{n=0}^{N-1} h(n) e^{-j\omega n} \tag{19}$$

and then

$$H(e^{j\frac{2\pi k}{N}}) = \sum_{n=0}^{N-1} h(n) e^{-j\frac{2\pi k n}{N}}, \text{ for } k = 0, 1, \ldots, (N-1) \tag{20}$$

FIR filter approximation by frequency sampling

- It is then natural to consider designing a length-N FIR filter by finding an $h(n)$ whose DFT corresponds exactly to samples of the desired frequency response.

- In other words, $h(n)$ can be determined by sampling the desired frequency response at the N points $e^{j\frac{2\pi}{N}k}$ and finding its inverse DFT. This method is generally referred to as the frequency sampling approach.

- More precisely, if the desired frequency response is given by $D(\omega)$, one must first find

$$A(k)e^{j\theta(k)} = D\left(\frac{\omega_s k}{N}\right), \text{ for } k = 0, 1, \ldots, (N-1) \tag{21}$$

  where $A(k)$ and $\theta(k)$ are samples of the desired amplitude and phase responses, respectively.

FIR filter approximation by frequency sampling

- If we want the resulting filter to have linear phase, $h(n)$ must be of one of the forms given in Subsection 4.2.3. For each form, the functions $A(k)$ and $\theta(k)$ present particular properties.

- We then summarize the results for these four cases separately.

- Obs.: To maintain consistency with the notation in Subsection 4.2.3, in the following discussion we will use the filter order $M = N - 1$ instead of the filter length N.

FIR filter approximation by frequency sampling

- Type I: Even order M and symmetrical impulse response. In this case, the phase and amplitude responses must satisfy

$$\theta(k) = -\frac{\pi k M}{M+1}, \text{ for } 0 \leq k \leq M \tag{22}$$

$$A(k) = A(M-k+1), \text{ for } 1 \leq k \leq \frac{M}{2} \tag{23}$$

and then, the impulse response is given by

$$h(n) = \frac{1}{M+1}\left[A(0) + 2\sum_{k=1}^{\frac{M}{2}}(-1)^k A(k)\cos\frac{\pi k(1+2n)}{M+1}\right] \tag{24}$$

for $n = 0, 1, \ldots, M$.

FIR filter approximation by frequency sampling

- Type II: Odd order M and symmetrical impulse response. The phase and amplitude responses, in this case, become

$$\theta(k) = \begin{cases} -\dfrac{\pi k M}{M+1}, & \text{for } 0 \leq k \leq \frac{M-1}{2} \\ \pi - \dfrac{\pi k M}{M+1}, & \text{for } \frac{M+3}{2} \leq k \leq M \end{cases} \tag{25}$$

$$A(k) = A(M-k+1), \text{ for } 1 \leq k \leq \tfrac{M+1}{2} \tag{26}$$

$$A\left(\frac{M+1}{2}\right) = 0 \tag{27}$$

and the impulse response is

$$h(n) = \frac{1}{M+1}\left[A(0) + 2\sum_{k=1}^{\frac{M-1}{2}} (-1)^k A(k) \cos\frac{\pi k(1+2n)}{M+1}\right] \tag{28}$$

for $n = 0, 1, \ldots, M$.

FIR filter approximation by frequency sampling

- Type III: Even order M and antisymmetric impulse response. The phase and amplitude responses are such that

$$\theta(k) = \frac{(1+2r)\pi}{2} - \frac{\pi k M}{M+1}, \text{ for } r \in \mathbb{Z} \text{ and } 0 \leq k \leq M \tag{29}$$

$$A(k) = A(M-k+1), \text{ for } 1 \leq k \leq \frac{M}{2} \tag{30}$$

$$A(0) = 0 \tag{31}$$

and the impulse response is given by

$$h(n) = \frac{2}{M+1} \sum_{k=1}^{\frac{M}{2}} (-1)^{k+1} A(k) \sin \frac{\pi k(1+2n)}{M+1} \tag{32}$$

for $n = 0, 1, \ldots, M$.

FIR filter approximation by frequency sampling

- Type IV: Odd order M and antisymmetric impulse response. In this case, the phase and amplitude responses are of the form

$$\theta(k) = \begin{cases} \dfrac{\pi}{2} - \dfrac{\pi k M}{M+1}, & \text{for } 1 \leq k \leq \frac{M-1}{2} \\ -\dfrac{\pi}{2} - \dfrac{\pi k M}{M+1}, & \text{for } \frac{M+1}{2} \leq k \leq M \end{cases} \tag{33}$$

$$A(k) = A(M-k+1), \qquad \text{for } 1 \leq k \leq M \tag{34}$$

$$A(0) = 0 \tag{35}$$

and the impulse response then becomes

$$h(n) = \frac{1}{M+1}\left[(-1)^{\frac{M+1}{2}+n} A\left(\frac{M+1}{2}\right) + 2\sum_{k=1}^{\frac{M-1}{2}} (-1)^k A(k) \sin\frac{\pi k(1+2n)}{M+1}\right] \tag{36}$$

for $n = 0, 1, \ldots, M$.

Table 2: Impulse responses for linear-phase FIR filters with frequency sampling approach.

Filter type	Impulse response $h(n)$, for $n = 0, 1, \ldots, M$	Condition
Type I	$\frac{1}{M+1}\left[A(0) + 2\sum_{k=1}^{\frac{M}{2}} (-1)^k A(k) \cos\frac{\pi k(1+2n)}{M+1}\right]$	
Type II	$\frac{1}{M+1}\left[A(0) + 2\sum_{k=1}^{\frac{M-1}{2}} (-1)^k A(k) \cos\frac{\pi k(1+2n)}{M+1}\right]$	$A\left(\frac{M+1}{2}\right) = 0$
Type III	$\frac{2}{M+1}\sum_{k=1}^{\frac{M}{2}} (-1)^{k+1} A(k) \sin\frac{\pi k(1+2n)}{M+1}$	$A(0) = 0$
Type IV	$\frac{1}{M+1}\left[(-1)^{\frac{M+1}{2}+n} A\left(\frac{M+1}{2}\right) + 2\sum_{k=1}^{\frac{M-1}{2}} (-1)^k A(k) \sin\frac{\pi k(1+2n)}{M+1}\right]$	$A(0) = 0$

Example 5.1

- Design a lowpass filter satisfying the specification below using the frequency sampling method:

$$\left.\begin{aligned} M &= 52 \\ \Omega_p &= 4.0 \text{ rad/s} \\ \Omega_r &= 4.2 \text{ rad/s} \\ \Omega_s &= 10.0 \text{ rad/s} \end{aligned}\right\} \tag{37}$$

- Obs.: Note that in this text, in general, the variable Ω represents an analog frequency, and the variable ω a digital frequency.

Example 5.1 - Solution

- We divide the $[0, \Omega_s]$ interval into $(M+1) = 53$ sub-intervals of same length $\frac{\Omega_s}{M+1}$, each starting at $\Omega_k = \frac{\Omega_s}{M+1}k$, for $k = 0, 1, \ldots, M$.

- According to the prescribed specifications, Ω_p and Ω_r lie close to the extremes

$$k_p = \left\lfloor (M+1) \times \frac{\Omega_p}{\Omega_s} \right\rfloor = \lfloor 53 \times \frac{4}{10} \rfloor = 21 \tag{38}$$

$$k_r = \left\lfloor (M+1) \times \frac{\Omega_r}{\Omega_s} \right\rfloor = \lfloor 53 \times \frac{4.2}{10} \rfloor = 22 \tag{39}$$

- Thus, we assign

$$A(k) = \begin{cases} 1, & \text{for } 0 \leq k \leq k_p \\ 0, & \text{for } k_r \leq k \leq \frac{M}{2} \end{cases} \tag{40}$$

Example 5.1 - Solution

- Then, one can employ the following MATLAB script, implementing the first row in Table 2, to design a Type I lowpass filter using the frequency sampling method:

```
M = 52; N = M+1;
Omega_p = 4; Omega_r = 4.2; Omega_s = 10;
kp = floor(N*Omega_p/Omega_s);
kr = floor(N*Omega_r/Omega_s);
A = [ones(1,kp+1) zeros(1,M/2-kr+1)];
k = 1:M/2;
for n=0:M,
  h(n+1) = A(1) +
2*sum((-1).^k.*A(k+1).*cos(pi.*k*(1+2*n)/N));
end;
h = h./N;
```

- Using this script, one ends up with the set of coefficients shown in Table 3.

Example 5.1 - Solution

Table 3: Coefficients of the lowpass filter designed with the frequency sampling method.

$h(0)$ to $h(26)$			
$h(0) = -0.0055$	$h(7) = -0.0202$	$h(14) = -0.0213$	$h(21) = 0.0114$
$h(1) = 0.0147$	$h(8) = 0.0204$	$h(15) = 0.0073$	$h(22) = -0.0560$
$h(2) = -0.0190$	$h(9) = -0.0135$	$h(16) = 0.0118$	$h(23) = 0.1044$
$h(3) = 0.0169$	$h(10) = 0.0014$	$h(17) = -0.0301$	$h(24) = -0.1478$
$h(4) = -0.0089$	$h(11) = 0.0124$	$h(18) = 0.0413$	$h(25) = 0.1779$
$h(5) = -0.0024$	$h(12) = -0.0231$	$h(19) = -0.0396$	$h(26) = 0.8113$
$h(6) = 0.0133$	$h(13) = 0.0268$	$h(20) = 0.0218$	

Example 5.1 - Solution

- The corresponding magnitude response is shown in Figure 4.

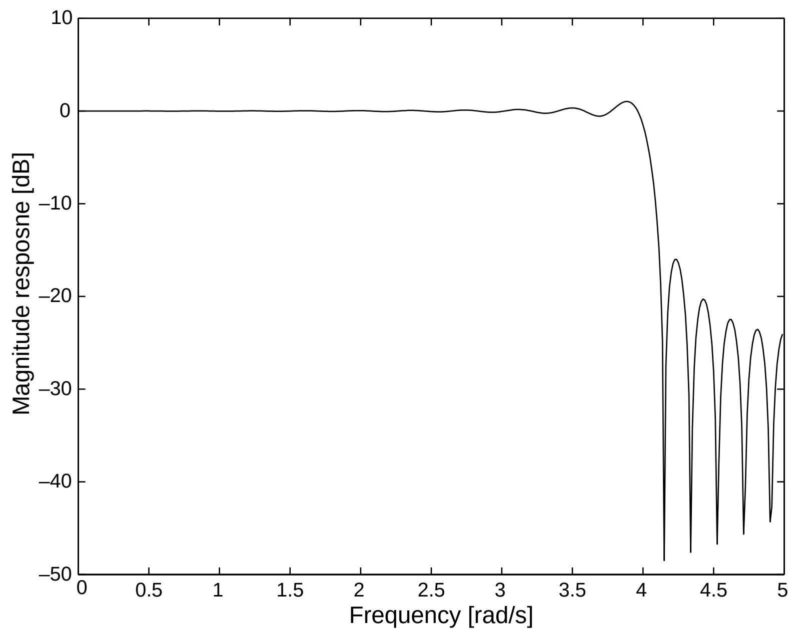

Figure 4: Magnitude response of the lowpass filter designed with the frequency sampling method.

FIR filter approximation by frequency sampling

- By examining the magnitude response shown in Figure 4, one notices that there is a great deal of ripple both at the passband and at the stopband. This is the main reason why this method has not found widespread use in filter design.

- This is not a surprising result, because the equations derived in this section guarantee only that the Fourier transform of $h(n)$ and the desired frequency response $D(\omega)$ (expressed as a function of the digital frequencies, that is, $\omega = 2\pi\frac{\Omega}{\Omega_s} = \Omega T$) coincide at the $M+1$ distinct frequencies $\frac{2\pi k}{M+1}$, for $k = 0, 1, \ldots, (M+1)$, where M is the filter order.

- At the other frequencies, as is illustrated in Figure 5, there is no constraint on the magnitude response, and, as a consequence, no control over the ripple δ.

FIR filter approximation by frequency sampling

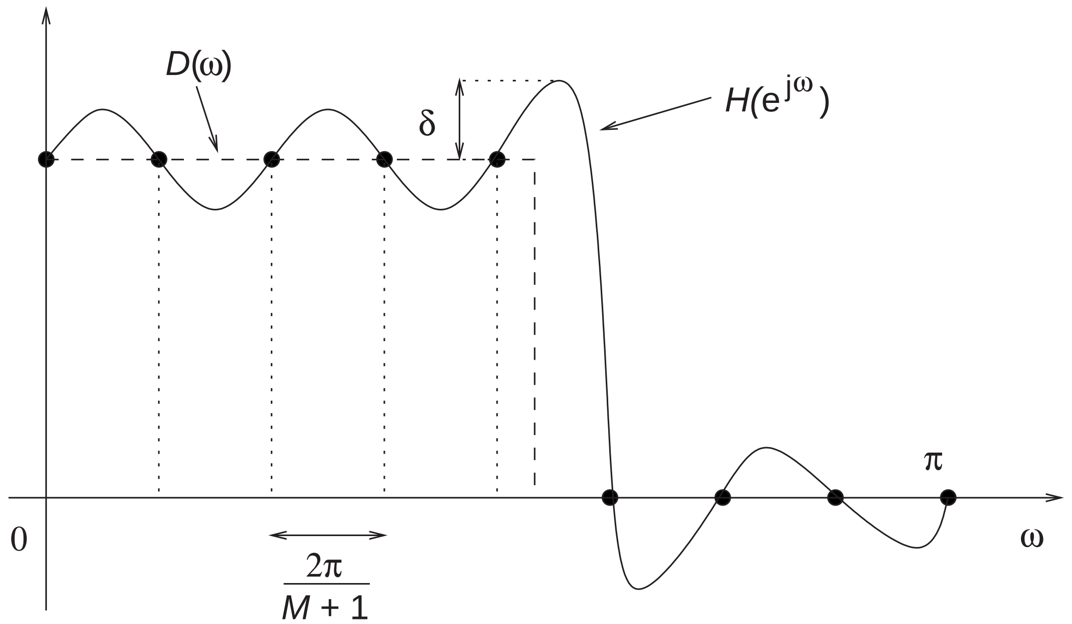

Figure 5: The desired magnitude response and the Fourier transform of $h(n)$ coincide only at the frequencies $\frac{2\pi k}{M+1}$, when using the frequency sampling approximation method.

FIR filter approximation by frequency sampling

- An interesting explanation of this fact comes from the expression of the inverse Fourier transform of the desired frequency response $D(\omega)$, which, from equation (3), is given by

$$h(n) = \frac{1}{2\pi}\int_{-\pi}^{\pi} D(\omega)e^{j\omega n}d\omega = \frac{1}{2\pi}\int_{0}^{2\pi} D(\omega)e^{j\omega n}d\omega \tag{41}$$

- If we try to approximate the above integral as a summation over the discrete frequencies $\frac{2\pi k}{N}$, by substituting $\omega \rightarrow \frac{2\pi k}{N}$ and $d\omega \rightarrow \frac{2\pi}{N}$, we end up with an approximation, $d(n)$, of $h(n)$ given by

$$d(n) = \frac{1}{2\pi}\sum_{n=0}^{N-1} D\left(\frac{2\pi k}{N}\right)e^{-j\frac{2\pi kn}{N}}\frac{2\pi}{N} = \frac{1}{N}\sum_{n=0}^{N-1} D\left(\frac{2\pi k}{N}\right)e^{-j\frac{2\pi kn}{N}} \tag{42}$$

- Hence, we see that $d(n)$ represents the IDFT of the sequence $D(\frac{2\pi k}{N})$, for $k = 0, 1, \ldots, (N-1)$.

FIR filter approximation by frequency sampling

- However, considering that the argument of the integral in equation (41) is $D(\omega)e^{j\omega n}$, the resolution of a good sampling grid for approximating it would have to be of the order of 10% of the period of the sinusoid $e^{j\omega n}$.

- This would require a sampling grid with a resolution of the order of $\frac{2\pi}{10N}$. In equation (42) we are approximating the integral using a sampling grid with resolution $\frac{2\pi}{N}$ and such approximation would only be valid for values of $n \leq \frac{N}{10}$.

- This is clearly not sufficient in most practical cases, which explains the large values of ripple depicted in Figure 4.

FIR filter approximation by frequency sampling

- One important situation, however, in which the frequency sampling method gives exact results is when the desired frequency response $D(\omega)$ is composed of a sum of sinusoids equally spaced in frequency. Such a result is formally stated in the following theorem.

- **Theorem:** If the desired frequency response $D(\omega)$ is a finite sum of complex sinusoids equally spaced in frequency, that is

$$D(\omega) = \sum_{n=N_0}^{N_1} a(n)e^{-j\omega n} \tag{43}$$

  then the frequency sampling method yields exact results, except for a constant group-delay term, provided that the length of the impulse response, N, satisfies $N \geq N_1 - N_0 + 1$.

FIR filter approximation by frequency sampling

- **Proof:** The theorem essentially states that the Fourier transform of the impulse response, $h(n)$, given by the frequency sampling method is identical to the desired frequency response $D(\omega)$, except for a constant group-delay term.

- That is, the above theorem is equivalent to

$$\mathcal{F}\left\{\text{IDFT}\left[D\left(\frac{2\pi k}{N}\right)\right]\right\} = D(\omega) \tag{44}$$

where $\mathcal{F}\{\cdot\}$ is the Fourier transform.

- The proof becomes simpler if we rewrite equation (44) as

$$D\left(\frac{2\pi k}{N}\right) = \text{DFT}\left\{\mathcal{F}^{-1}\left[D(\omega)\right]\right\} \tag{45}$$

for $k = 0, 1, \ldots, (N-1)$.

FIR filter approximation by frequency sampling

- For a desired frequency response in the form of equation (43), the corresponding inverse Fourier transform is given by

$$d(n) = \begin{cases} 0, & \text{for } n < N_0 \\ a(n), & \text{for } n = N_0, (N_0 + 1), \ldots, N_1 \\ 0, & \text{for } n > N_1 \end{cases} \tag{46}$$

- The length-N DFT of the length-N signal composed by the non-zero samples of $d(n)$, $H(k)$, is then equal to the length-N DFT of $a(n)$, adequately shifted in time to the interval $n \in [0, N-1]$.

FIR filter approximation by frequency sampling

- Therefore, if $N \geq N_1 - N_0 + 1$, we get that

$$
\begin{aligned}
H(k) &= \mathrm{DFT}\left[a(n' + N_0)\right] \\
&= \sum_{n'=0}^{N-1} a(n' + N_0) e^{-j\frac{2\pi k}{N}n'} \\
&= \sum_{n'=0}^{N-1} d(n' + N_0) e^{-j\frac{2\pi k}{N}n'} \\
&= \sum_{n=N_0}^{N+N_0-1} d(n) e^{-j\frac{2\pi k}{N}(n-N_0)} \\
&= e^{j\frac{2\pi k}{N}N_0} \sum_{n=N_0}^{N_1} d(n) e^{-j\frac{2\pi k}{N}n} \\
&= e^{j\frac{2\pi k}{N}N_0} D\left(\frac{2\pi k}{N}\right)
\end{aligned}
\tag{47}
$$

for $k = 0, 1, \ldots, (N-1)$, and this completes the proof.

FIR filter approximation by frequency sampling

- This result is very useful whenever the desired frequency response $D(\omega)$ is of the form described by equation (43), as is the case in the approximation methods discussed in Section 5.5 and Subsection 5.6.2.

FIR filter approximation with window functions

- For all ideal filters analyzed in Section 5.2, the impulse responses obtained from equation (3) have infinite duration, which leads to non-realizable FIR filters.
- A straightforward way to overcome this limitation is to define a finite-length auxiliary sequence $h'(n)$, yielding a filter of order M, as

$$h'(n) = \begin{cases} h(n), & \text{for } |n| \leq \frac{M}{2} \\ 0, & \text{for } |n| > \frac{M}{2} \end{cases} \tag{48}$$

assuming that M is even.

FIR filter approximation with window functions

- The resulting transfer function is written as

$$H'(z) = h(0) + \sum_{n=1}^{\frac{M}{2}} \left(h(-n)z^{n} + h(n)z^{-n} \right) \qquad (49)$$

- This is still a noncausal function which we can make causal by multiplying it by $z^{\frac{-M}{2}}$, without either distorting the filter magnitude response or destroying the linear-phase property.

- The example below highlights some of the impacts that the truncation of the impulse response in equations (48) and (49) has on the filter frequency response.

Example 5.2

- Design a bandstop filter satisfying the specification below:

$$\left.\begin{array}{lcl} M & = & 50 \\ \Omega_{c_1} & = & \frac{\pi}{4}\ \text{rad/s} \\ \Omega_{c_2} & = & \frac{\pi}{2}\ \text{rad/s} \\ \Omega_s & = & 2\pi\ \text{rad/s} \end{array}\right\} \qquad (50)$$

Example 5.2 - Solution

- Applying equations (48) and (49) to the corresponding bandstop equations in Table 1, one may use the script:

```
M = 50;
wc1 = pi/4; wc2 = pi/2; ws = 2*pi;
n = 1:M/2;
h0 = 1 - (wc2 - wc1)/pi;
haux = (sin(wc1.*n) - sin(wc2.*n))./(pi.*n);
h = [fliplr(haux) h0 haux];
```

  to obtain the filter coefficients listed in Table 4 (only half of them are listed as the others can be found using $h(n) = h(50 - n)$).

- The resulting magnitude response is depicted in Figure 6.

Example 5.2 - Solution

Table 4: Bandstop filter coefficients.

$h(0)$ to $h(25)$			
$h(0) = -0.0037$	$h(7) = 0.0177$	$h(14) = 0.0494$	$h(21) = 0.0000$
$h(1) = 0.0000$	$h(8) = -0.0055$	$h(15) = 0.0318$	$h(22) = 0.1811$
$h(2) = 0.0041$	$h(9) = 0.0000$	$h(16) = -0.0104$	$h(23) = 0.1592$
$h(3) = -0.0145$	$h(10) = 0.0062$	$h(17) = 0.0000$	$h(24) = -0.0932$
$h(4) = -0.0259$	$h(11) = -0.0227$	$h(18) = 0.0133$	$h(25) = 0.7500$
$h(5) = 0.0000$	$h(12) = -0.0418$	$h(19) = -0.0531$	
$h(6) = 0.0286$	$h(13) = 0.0000$	$h(20) = -0.1087$	

Example 5.2 - Solution

(a) (b)

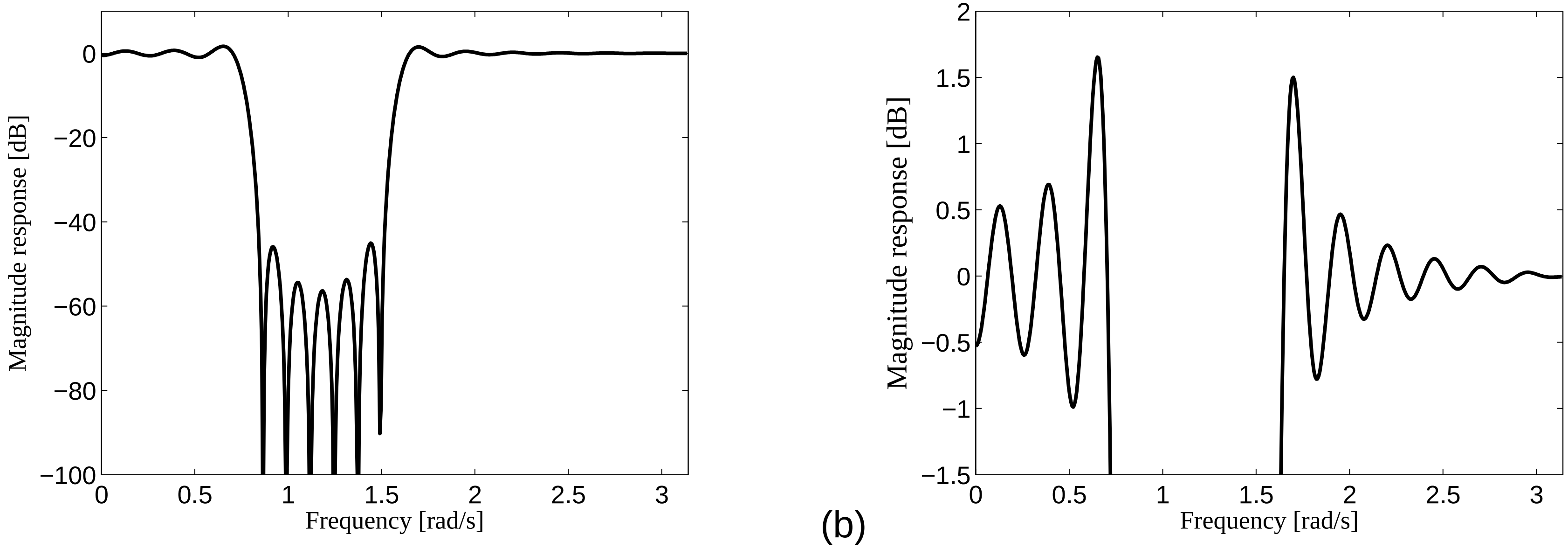

Figure 6: Bandstop filter: (a) magnitude response; (b) passband detail.

FIR filter approximation with window functions

- The ripple seen in Figure 6 close to the band edges is due to the slow convergence of the Fourier series $h(n)$ when approximating functions presenting discontinuities, such as the ideal responses seen in Figure 1.
- This implies that large amplitude ripples in the magnitude response appear close to the edges whenever an infinite-length $h(n)$ is truncated to generate a finite-length filter. These ripples are commonly referred to as Gibbs' oscillations.
- It can be shown that Gibbs' oscillations possess the property that their amplitudes do not decrease even when the filter order M is increased dramatically. This severely limits the practical usefulness of equations (48) and (49) in FIR design, because the maximum deviation from the ideal magnitude response can not be minimized by increasing the filter length.

FIR filter approximation with window functions

- Although we can not remove the ripples introduced by the poor convergence of the Fourier series, we can still attempt to control their amplitude by multiplying the impulse response $h(n)$ by a window function $w(n)$.

- The window $w(n)$ must be designed such that it introduces minimum deviation from the ideal frequency response. The coefficients of the resulting impulse response $h'(n)$ become

$$h'(n) = h(n)w(n) \tag{51}$$

- In the frequency domain, such a multiplication corresponds to a periodic convolution operation between the frequency responses of the ideal filter, $H(e^{j\omega})$, and of the window function, $W(e^{j\omega})$, that is

$$H'(e^{j\omega}) = \frac{1}{2\pi}\int_{-\pi}^{\pi} H(e^{j\omega'})W(e^{j(\omega-\omega')})d\omega' \tag{52}$$

FIR filter approximation with window functions

- We can then infer that a good window is a finite-length sequence, whose frequency response, when convolved with an ideal frequency response, produces the minimum distortion possible.

- This minimum distortion would occur when the frequency response of the window has an impulse-like shape, concentrated around $\omega = 0$, as depicted in Figure 7a.

- However, band-limited signals in frequency are not limited in time, and therefore such a window sequence would have to be infinite, which contradicts our main requirement. This means that we must find a finite-length window which has a frequency response that has most of its energy concentrated around $\omega = 0$.

- Also, in order to avoid the oscillations in the filter magnitude response, the sidelobes of the window magnitude response should quickly decay as $|\omega|$ is increased.

FIR filter approximation with window functions

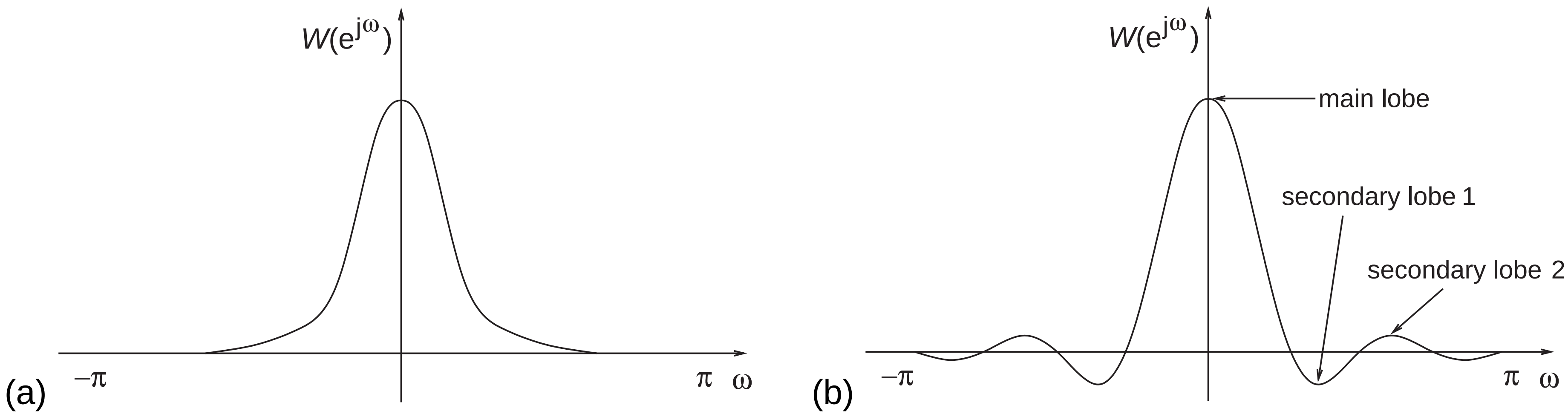

Figure 7: Magnitude responses of a window function: (a) ideal case; (b) practical case.

FIR filter approximation with window functions

- A practical window function is in general as shown in Figure 7b. The effect of the secondary lobe is to introduce the largest ripple close to the band edges.
- From equation (52), we see that the main-lobe width determines the transition bandwidth of the resulting filter.
- Based on these facts, a practical window function must present a magnitude response characterized by:
  - The ratio of the main-lobe amplitude to the secondary-lobe amplitude must be as large as possible.
  - The energy must decay rapidly when $|\omega|$ increases from 0 to π.
- We can now proceed to perform a thorough study of the more widely used window functions in FIR filter design.

Rectangular window

- A simple truncation of the impulse response as described in equation (48) can be interpreted as the product between the ideal $h(n)$ and a window given by

$$w_r(n) = \begin{cases} 1, & \text{for } |n| \leq \frac{M}{2} \\ \\ 0, & \text{for } |n| > \frac{M}{2} \end{cases} \tag{53}$$

- Note that if we want to truncate the impulse responses in Table 1 using the above equation, and still keep the linear-phase property, the resulting truncated sequences would have to be either symmetric or antisymmetric around $n = 0$.

- This implies that, for those cases, M would have to be even (Type-I and Type-III filters, as seen in Subsection 4.2.3).

- For the case of M odd, the solution would be to shift $h(n)$ so that it is causal and apply a window different from zero from $n = 0$ to $n = M - 1$. This solution, however, is not commonly used in practice.

Rectangular window

- From equation (53), the frequency response of the rectangular window is given by

$$
\begin{aligned}
W_r(e^{j\omega}) &= \sum_{n=-\frac{M}{2}}^{\frac{M}{2}} e^{-j\omega n} \\
&= \frac{e^{j\omega\frac{M}{2}} - e^{-j\omega\frac{M}{2}}e^{-j\omega}}{1 - e^{-j\omega}} \\
&= e^{-j\frac{\omega}{2}} \frac{\left[e^{j\omega\left(\frac{M+1}{2}\right)} - e^{-j\omega\left(\frac{M+1}{2}\right)}\right]}{1 - e^{-j\omega}} \\
&= \frac{\sin\left[\omega\left(\frac{M+1}{2}\right)\right]}{\sin\left(\frac{\omega}{2}\right)} \qquad (54)
\end{aligned}
$$

Triangular windows

- The main problem associated with the rectangular window is the presence of ripples near the band edges of the resulting filter, which are caused by the existence of sidelobes in the frequency response of the window.

- Such a problem is due to the inherent discontinuity of the rectangular window in the time domain. One way to reduce such a discontinuity is to employ a triangular-shaped window, which will present only small discontinuities near its edges.

- The standard triangular window is defined as

$$w_t(n) = \begin{cases} -\dfrac{2|n|}{M+2} + 1, & \text{for } |n| \leq \frac{M}{2} \\ 0, & \text{for } |n| > \frac{M}{2} \end{cases} \tag{55}$$

Triangular windows

- A small variation of such a window is called the Bartlett window and is defined by

$$w_{tB}(n) = \begin{cases} -\dfrac{2|n|}{M} + 1, & \text{for } |n| \leq \frac{M}{2} \\ 0, & \text{for } |n| > \frac{M}{2} \end{cases} \tag{56}$$

- These two triangular-type window functions are closely related. Their main difference lies in the fact that the Bartlett window presents one null element at each of its extremities. In that manner, an Mth-order Bartlett window can be obtained by juxtaposing one zero at each extremity of the $(M-2)$th-order standard triangular window.

- In some cases, an even greater reduction of the sidelobes is necessary, and then more complex window functions should be used, such as the ones described below.

Hamming and Hann windows

- The generalized Hamming window is defined as

$$w_H(n) = \begin{cases} \alpha + (1-\alpha)\cos\left(\frac{2\pi n}{M}\right), & \text{for } |n| \leq \frac{M}{2} \\ 0, & \text{for } |n| > \frac{M}{2} \end{cases} \tag{57}$$

with $0 \leq \alpha \leq 1$.

- This generalized window is referred to as the Hamming window when $\alpha = 0.54$, and for $\alpha = 0.5$, it is known as the Hann or Hanning window.

- The frequency response for the general Hamming window can be expressed based on the frequency response of the rectangular window.

Hamming and Hann windows

- We first write equation (57) as

$$w_H(n) = w_r(n)\left[\alpha + (1-\alpha)\cos\left(\frac{2\pi n}{M}\right)\right] \tag{58}$$

- By transforming the above equation to the frequency domain, clearly the frequency response of the generalized Hamming window results from the periodic convolution between $W_r(e^{j\omega})$ and three impulse functions as

$$W_H(e^{j\omega}) = W_r(e^{j\omega}) * \left[\alpha\delta(\omega) + \left(\frac{1-\alpha}{2}\right)\delta\left(\omega - \frac{2\pi}{M}\right) + \left(\frac{1-\alpha}{2}\right)\delta\left(\omega + \frac{2\pi}{M}\right)\right] \tag{59}$$

- And then

$$W_H(e^{j\omega}) = \alpha W_r(e^{j\omega}) + \left(\frac{1-\alpha}{2}\right)W_r\left(e^{j(\omega - \frac{2\pi}{M})}\right) + \left(\frac{1-\alpha}{2}\right)W_r\left(e^{j(\omega + \frac{2\pi}{M})}\right) \tag{60}$$

Hamming and Hann windows

- From this equation, one notices that $W_{\mathrm{H}}(\mathrm{e}^{\mathrm{j}\omega})$ is composed of three versions of the rectangular spectrum $W_{\mathrm{r}}(\mathrm{e}^{\mathrm{j}\omega})$: the main component, $\alpha W_{\mathrm{r}}(\mathrm{e}^{\mathrm{j}\omega})$, centered at $\omega = 0$, and two additional ones with smaller amplitudes, centered at $\omega = \pm 2\pi/M$, that reduce the secondary lobe of the main component.

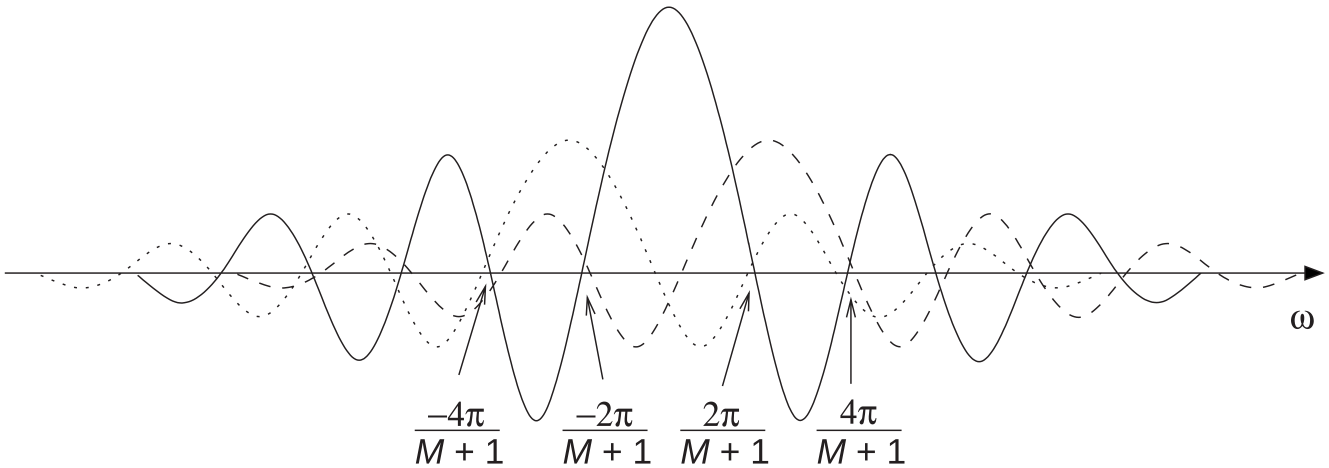

Figure 8: The three components of the generalized Hamming window combine to reduce the resulting secondary lobes. (Solid line – $\alpha W_{\mathrm{r}}(\mathrm{e}^{\mathrm{j}\omega})$; dashed line – $\frac{1-\alpha}{2} W_{\mathrm{r}}\left(\mathrm{e}^{\mathrm{j}(\omega - \frac{\pi}{M})}\right)$; dotted line – $\frac{1-\alpha}{2} W_{\mathrm{r}}\left(\mathrm{e}^{\mathrm{j}(\omega + \frac{\pi}{M})}\right)$.)

Hamming and Hann windows

- The main characteristics of the generalized Hamming window are:
  - All three $W_r(e^{j\omega})$ components have zeros close to $\omega = \pm\frac{4\pi}{M+1}$. Hence, the main-lobe total width is $\frac{8\pi}{M+1}$.
  - When $\alpha = 0.54$, the main-lobe total energy is approximately 99.96% of the window total energy.
  - The transition band of the Hamming window is larger than the transition band of the rectangular window, due to its wider main lobe.
  - The ratio between the amplitudes of the main and secondary lobes of the Hamming window is much larger than for the rectangular window.
  - The stopband attenuation for the Hamming window is larger than the attenuation for the rectangular window.

Blackman window

- The Blackman window is defined as

$$w_{B}(n) = \begin{cases} 0.42 + 0.5\cos\left(\frac{2\pi n}{M}\right) + 0.08\cos\left(\frac{4\pi n}{M}\right), & \text{for } |n| \leq \frac{M}{2} \\ 0, & \text{for } |n| > \frac{M}{2} \end{cases} \quad (61)$$

- Compared to the Hamming window function, the Blackman window introduces a second cosine term to further reduce the effects of the secondary lobes of $W_{r}(e^{j\omega})$.
- The Blackman window is characterized by the following issues:
  - The main-lobe width is approximately $\frac{12\pi}{M+1}$, which is wider than that for the previous windows.
  - The passband ripples are smaller than in the previous windows.
  - The stopband attenuation is larger than in the previous windows.

Example 5.3

- Design a bandstop filter satisfying the specification below using the rectangular, Hamming, Hann, and Blackman windows:

$$\left.\begin{aligned} M &= 80 \\ \Omega_{p_1} &= 2000 \text{ rad/s} \\ \Omega_{p_2} &= 4000 \text{ rad/s} \\ \Omega_s &= 10\,000 \text{ rad/s} \end{aligned}\right\} \tag{62}$$

Example 5.3 - Solution

- This time, filter specifications are given in the analog frequency domain. Hence, one must first normalize Ω_{p_1} and Ω_{p_2} before employing a script similar to the one given in Example 5.2:

```
M = 80;
Omega_c1 = 2000; Omega_c2 = 4000; Omega_s = 10000;
wc1 = Omega_c1*2*pi/Omega_s; wc2 =
Omega_c2*2*pi/Omega_s;
n = 1:M/2;
h0 = 1 - (wc2 - wc1)/pi;
haux = (sin(wc1.*n) - sin(wc2.*n))./(pi.*n);
h = [fliplr(haux) h0 haux];
```

to obtain the impulse response using the rectangular window.

Example 5.3 - Solution

- For the other three windows, one must multiply sample-by-sample $h(n)$ above by the corresponding window obtained with the MATLAB commands `hamming(M+1);`, `hanning(M+1);`, and `blackman(M+1);`.

- The resulting impulse responses are shown in Tables 5–8, where only the filter coefficients for $0 \leq n \leq 40$ are given, since the remaining coefficients can be obtained as $h(n) = h(80 - n)$.

- The magnitude responses associated to the four impulse responses listed in Tables 5–8 are depicted in Figure 9. The reader should notice the compromise between the transition bandwidth and the ripple in the passband and stopband when going from the rectangular to the Blackman window, that is, as the ripple decreases, the width of the transition band increases accordingly.

Example 5.3 - Solution

Table 5: Filter coefficients using the rectangular window.

$h(0)$ to $h(40)$			
$h(0) = 0.0000$	$h(11) = -0.0040$	$h(22) = -0.0272$	$h(33) = 0.0700$
$h(1) = -0.0030$	$h(12) = -0.0175$	$h(23) = 0.0288$	$h(34) = 0.0193$
$h(2) = -0.0129$	$h(13) = 0.0181$	$h(24) = 0.0072$	$h(35) = 0.0000$
$h(3) = 0.0132$	$h(14) = 0.0044$	$h(25) = 0.0000$	$h(36) = -0.0289$
$h(4) = 0.0032$	$h(15) = 0.0000$	$h(26) = -0.0083$	$h(37) = -0.1633$
$h(5) = 0.0000$	$h(16) = -0.0048$	$h(27) = -0.0377$	$h(38) = 0.2449$
$h(6) = -0.0034$	$h(17) = -0.0213$	$h(28) = 0.0408$	$h(39) = 0.1156$
$h(7) = -0.0148$	$h(18) = 0.0223$	$h(29) = 0.0105$	$h(40) = 0.6000$
$h(8) = 0.0153$	$h(19) = 0.0055$	$h(30) = 0.0000$	
$h(9) = 0.0037$	$h(20) = 0.0000$	$h(31) = -0.0128$	
$h(10) = 0.0000$	$h(21) = -0.0061$	$h(32) = -0.0612$	

Example 5.3 - Solution

Table 6: Filter coefficients using the Hamming window.

$h(0)$ to $h(40)$			
$h(0) = 0.0000$	$h(11) = -0.0010$	$h(22) = -0.0167$	$h(33) = 0.0652$
$h(1) = -0.0002$	$h(12) = -0.0047$	$h(23) = 0.0187$	$h(34) = 0.0183$
$h(2) = -0.0011$	$h(13) = 0.0054$	$h(24) = 0.0049$	$h(35) = 0.0000$
$h(3) = 0.0012$	$h(14) = 0.0015$	$h(25) = 0.0000$	$h(36) = -0.0283$
$h(4) = 0.0003$	$h(15) = 0.0000$	$h(26) = -0.0062$	$h(37) = -0.1612$
$h(5) = 0.0000$	$h(16) = -0.0019$	$h(27) = -0.0294$	$h(38) = 0.2435$
$h(6) = -0.0004$	$h(17) = -0.0092$	$h(28) = 0.0331$	$h(39) = 0.1155$
$h(7) = -0.0022$	$h(18) = 0.0104$	$h(29) = 0.0088$	$h(40) = 0.6000$
$h(8) = 0.0026$	$h(19) = 0.0028$	$h(30) = 0.0000$	
$h(9) = 0.0007$	$h(20) = 0.0000$	$h(31) = -0.0114$	
$h(10) = 0.0000$	$h(21) = -0.0035$	$h(32) = -0.0558$	

Example 5.3 - Solution

Table 7: Filter coefficients using the Hann window.

$h(0)$ to $h(40)$			
$h(0) = 0.0000$	$h(11) = -0.0008$	$h(22) = -0.0162$	$h(33) = 0.0651$
$h(1) = -0.0000$	$h(12) = -0.0040$	$h(23) = 0.0182$	$h(34) = 0.0183$
$h(2) = -0.0002$	$h(13) = 0.0047$	$h(24) = 0.0048$	$h(35) = 0.0000$
$h(3) = 0.0003$	$h(14) = 0.0013$	$h(25) = 0.0000$	$h(36) = -0.0282$
$h(4) = 0.0001$	$h(15) = 0.0000$	$h(26) = -0.0061$	$h(37) = -0.1611$
$h(5) = 0.0000$	$h(16) = -0.0018$	$h(27) = -0.0291$	$h(38) = 0.2435$
$h(6) = -0.0002$	$h(17) = -0.0086$	$h(28) = 0.0328$	$h(39) = 0.1155$
$h(7) = -0.0014$	$h(18) = 0.0099$	$h(29) = 0.0088$	$h(40) = 0.6000$
$h(8) = 0.0017$	$h(19) = 0.0026$	$h(30) = 0.0000$	
$h(9) = 0.0005$	$h(20) = 0.0000$	$h(31) = -0.0114$	
$h(10) = 0.0000$	$h(21) = -0.0034$	$h(32) = -0.0557$	

Example 5.3 - Solution

Table 8: Filter coefficients using the Blackman window.

$h(0)$ to $h(40)$			
$h(0) = 0.0000$	$h(11) = -0.0003$	$h(22) = -0.0115$	$h(33) = 0.0618$
$h(1) = -0.0000$	$h(12) = -0.0018$	$h(23) = 0.0134$	$h(34) = 0.0176$
$h(2) = -0.0000$	$h(13) = 0.0022$	$h(24) = 0.0037$	$h(35) = 0.0000$
$h(3) = 0.0001$	$h(14) = 0.0006$	$h(25) = 0.0000$	$h(36) = -0.0278$
$h(4) = 0.0000$	$h(15) = 0.0000$	$h(26) = -0.0050$	$h(37) = -0.1596$
$h(5) = 0.0000$	$h(16) = -0.0010$	$h(27) = -0.0243$	$h(38) = 0.2424$
$h(6) = -0.0001$	$h(17) = -0.0049$	$h(28) = 0.0281$	$h(39) = 0.1153$
$h(7) = -0.0004$	$h(18) = 0.0059$	$h(29) = 0.0077$	$h(40) = 0.6000$
$h(8) = 0.0006$	$h(19) = 0.0017$	$h(30) = 0.0000$	
$h(9) = 0.0002$	$h(20) = 0.0000$	$h(31) = -0.0104$	
$h(10) = 0.0000$	$h(21) = -0.0023$	$h(32) = -0.0520$	

Example 5.3 - Solution

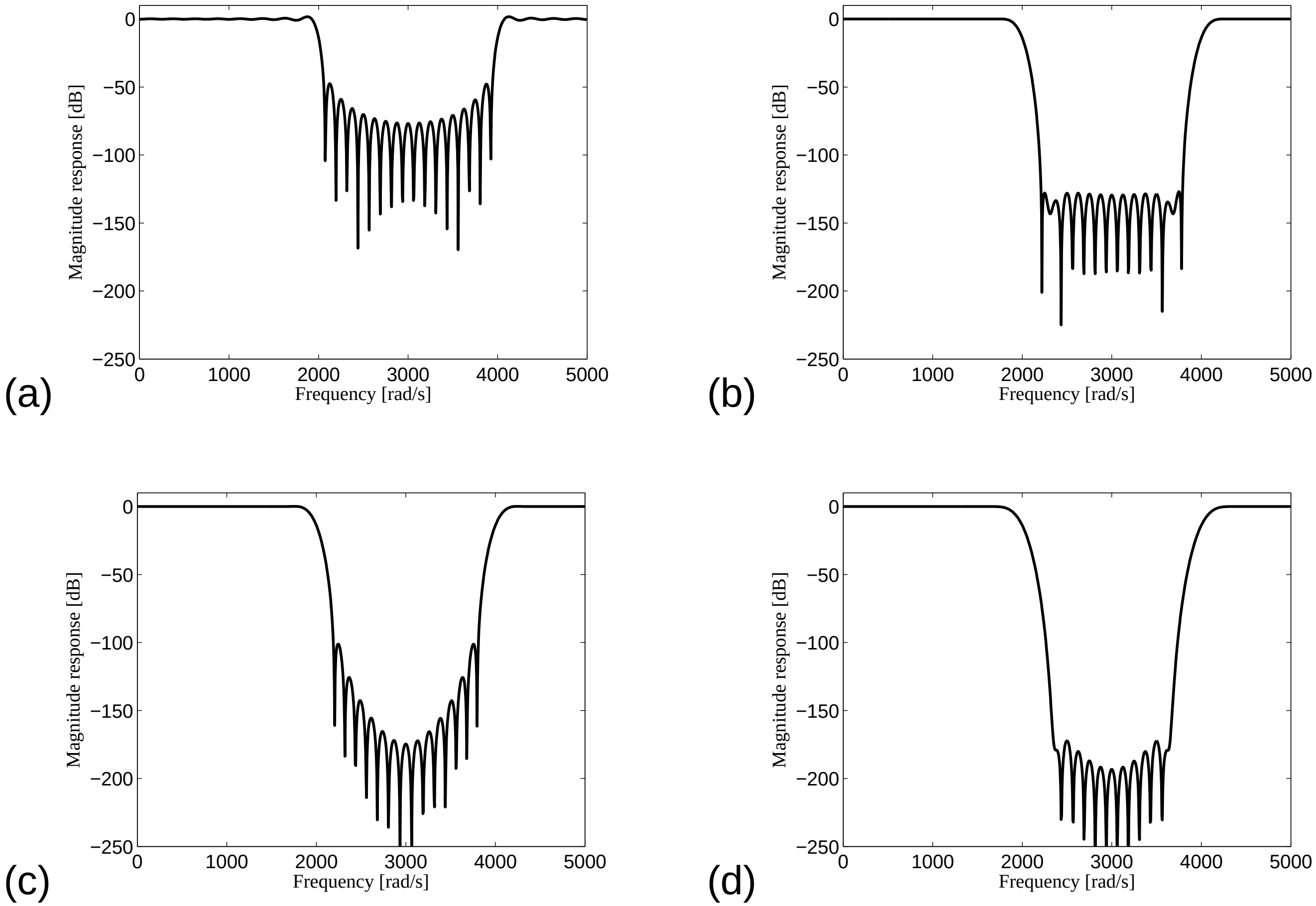

Figure 9: Magnitude responses when using: (a) rectangular; (b) Hamming; (c) Hann; (d) Blackman windows.

Kaiser window

- All the window functions seen so far allow us to control the transition band through a proper choice of the filter order M.
- However, no control can be achieved over the passband and stopband ripples, which makes these windows of little use when designing filters with prescribed frequency specifications, such as that depicted in Figure 10.
- Such problems are overcome with the Kaiser and Dolph-Chebyshev windows, presented in this and in the next subsections.

Kaiser window

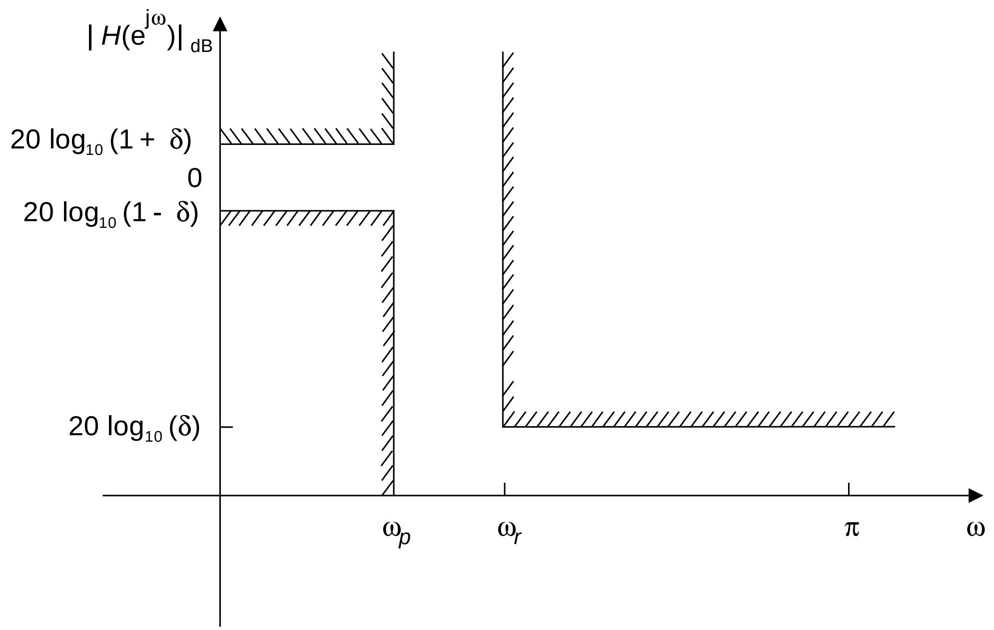

Figure 10: Typical specification of a lowpass filter. The specifications are in terms of the digital frequency $\omega = 2\pi\frac{\Omega}{\Omega_s} = \Omega T$.

Kaiser window

- As seen earlier in this section, the ideal window should be a finite-duration function such that most of its spectral energy is concentrated around $|\omega| = 0$, quickly decaying when $|\omega|$ increases.
- There is a family of continuous-time functions, called the prolate spheroidal functions, which are optimal for achieving these properties.

Kaiser window

- Such functions, although very difficult to implement in practice, can be effectively approximated with the hyperbolic-sine $I_0(\cdot)$ functions as

$$w(t) = \begin{cases} \dfrac{I_0\left[\beta\sqrt{1-(\frac{t}{\tau})^2}\right]}{I_0(\beta)}, & \text{for } |t| \leq \tau \\ 0, & \text{for } |t| > \tau \end{cases} \tag{63}$$

where $\beta = \Omega_a \tau$ and $I_0(x)$ is the zeroth-order modified Bessel function of the first kind, which can be efficiently determined through its series expansion given by

$$I_0(x) = 1 + \sum_{k=1}^{\infty} \left[\frac{(\frac{x}{2})^k}{k!}\right]^2 \tag{64}$$

Kaiser window

- The Fourier transform of $w(t)$ is given by

$$W(\Omega) = \frac{2\tau \sin\left[\beta\sqrt{(\frac{\Omega}{\Omega_a})^2 - 1}\right]}{\beta I_0(\beta)\sqrt{(\frac{\Omega}{\Omega_a})^2 - 1}} \tag{65}$$

- The Kaiser window is derived from equation (63) by making the transformation to the discrete-time domain given by $\tau \rightarrow \frac{M}{2}T$ and $t \rightarrow nT$. The window is then described by

$$w_K(n) = \begin{cases} \dfrac{I_0\left[\beta\sqrt{1 - (\frac{2n}{M})^2}\right]}{I_0(\beta)}, & \text{for } |n| \leq \frac{M}{2} \\ 0, & \text{for } |n| > \frac{M}{2} \end{cases} \tag{66}$$

- Since the functions given by equation (65) tend to be highly concentrated around $|\Omega| = 0$, we can assume that $W(\Omega) \approx 0$, for $|\Omega| \geq \frac{\Omega_s}{2}$.

Kaiser window

- Therefore, we can approximate the frequency response for the Kaiser window by

$$W_K(e^{j\omega}) \approx \frac{1}{T} W\left(\frac{\omega}{T}\right) \tag{67}$$

where $W(\Omega)$ is given by equation (65) when τ is replaced by $\frac{M}{2}T$.

- This yields

$$W_K(e^{j\omega}) \approx \frac{M \sin\left[\beta\sqrt{(\frac{\omega}{\omega_a})^2 - 1}\right]}{\beta I_0(\beta)\sqrt{(\frac{\omega}{\omega_a})^2 - 1}} \tag{68}$$

where $\omega_a = \Omega_a T$ and $\beta = \Omega_a \tau = \frac{\omega_a}{T}\frac{M}{2}T = \omega_a \frac{M}{2}$.

- The main advantage of the Kaiser window appears in the design of FIR digital filters with prescribed specifications, such as that depicted in Figure 10, where the parameter β is used to control some filter characteristics.

Kaiser window

- The overall procedure for designing FIR filters using the Kaiser window is as follows:
  - (i) From the ideal frequency response that the filter is supposed to approximate, determine the impulse response $h(n)$ using Table 1. If the filter is either lowpass or highpass, one should make $\Omega_c = \frac{\Omega_p + \Omega_r}{2}$. The case of bandpass and bandstop filters is dealt with later in this subsection.
  - (ii) Given the maximum passband ripple in dB, A_p, and the minimum stopband attenuation in dB, A_r, determine the corresponding ripples

$$\delta_p = \frac{10^{0.05A_p} - 1}{10^{0.05A_p} + 1} \tag{69}$$

$$\delta_r = 10^{-0.05A_r} \tag{70}$$

Kaiser window

- (cont.)
  - (iii) As with all other window functions, the Kaiser window can only be used to design filters that present the same passband and stopband ripples. Therefore, in order to satisfy the prescribed specifications, one should use $\delta = \min\{\delta_p, \delta_r\}$.
  - (iv) Compute the resulting passband ripple and stopband attenuation in dB using

$$A_p = 20 \log \frac{1+\delta}{1-\delta} \tag{71}$$

$$A_r = -20 \log \delta \tag{72}$$

  - (v) Given the passband and stopband edges, Ω_p and Ω_r, respectively, compute the transition bandwidth $T_r = (\Omega_r - \Omega_p)$.

Kaiser window

- (cont.)
  - (vi) Compute β using

$$\beta = \begin{cases} 0, & \text{for } A_r \leq 21 \\ 0.5842(A_r - 21)^{0.4} + 0.078\,86(A_r - 21), & \text{for } 21 < A_r \leq 50 \\ 0.1102(A_r - 8.7), & \text{for } 50 < A_r \end{cases} \quad (73)$$

    This empirical formula was devised by Kaiser based on the behavior of the function $W(\Omega)$ in equation (65).
  - (vii) Defining the normalized window length $D = \frac{T_r M}{\Omega_s}$, where Ω_s is the sampling frequency, we have that:

$$D = \begin{cases} 0.9222, & \text{for } A_r \leq 21 \\ \dfrac{(A_r - 7.95)}{14.36}, & \text{for } 21 < A_r \end{cases} \quad (74)$$

Kaiser window

- (cont.)
  - (viii) Having computed D using equation (74), we can determine the filter order M as the smallest even number that satisfies

$$M \geq \frac{\Omega_s D}{T_r} \tag{75}$$

One should remember that T_r must be in the same units as Ω_s.

  - (ix) With M and β determined, we compute the window $w_K(n)$ using equation (66). We are now ready to form the sequence $h'(n) = w_K(n)h(n)$, where $h(n)$ is the ideal filter impulse response computed in step (i).
  - (x) The desired transfer function is then given by

$$H(z) = z^{-\frac{M}{2}} \mathcal{Z}\{h'(n)\} \tag{76}$$

Kaiser window

- The above procedure applies to lowpass filters (see Figure 10) as well as highpass filters. If the filter is either bandpass or bandstop, we must include the following reasoning in step (i) above:
  - 1. Compute the narrower transition band

$$T_r = \pm \text{min}\{|\Omega_{r_1} - \Omega_{p_1}|, |\Omega_{p_2} - \Omega_{r_2}|\} \tag{77}$$

    Notice that T_r is negative for bandpass filters and positive for bandstop filters.
  - 2. Determine the two central frequencies as

$$\Omega_{c_1} = \left(\Omega_{p_1} + \frac{T_r}{2}\right) \tag{78}$$

$$\Omega_{c_2} = \left(\Omega_{p_2} - \frac{T_r}{2}\right) \tag{79}$$

Kaiser window

- A typical magnitude specification for a bandstop filter is depicted in Figure 11.

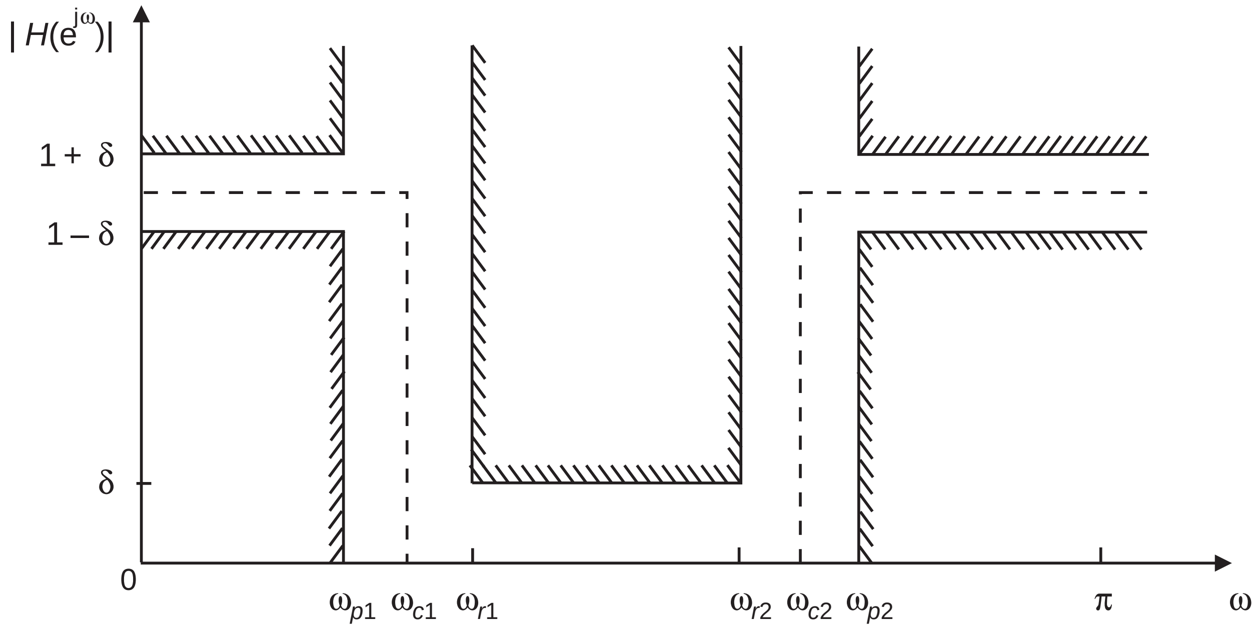

Figure 11: Typical specification of a bandstop filter.

Example 5.4

- Design a bandstop filter satisfying the specification below using the Kaiser window:

$$\left.\begin{aligned} A_p &= 1.0 \text{ dB} \\ A_r &= 45 \text{ dB} \\ \Omega_{p_1} &= 800 \text{ Hz} \\ \Omega_{r_1} &= 950 \text{ Hz} \\ \Omega_{r_2} &= 1050 \text{ Hz} \\ \Omega_{p_2} &= 1200 \text{ Hz} \\ \Omega_s &= 6000 \text{ Hz} \end{aligned}\right\} \qquad (80)$$

CAMBRIDGE UNIVERSITY PRESS

Example 5.4 - Solution

- Following the procedure described above, the resulting filter is obtained as follows (note that in the FIR design procedure described above, the parameters of the Kaiser window depend only on the ratio of the analog frequencies in the filter specification to the sampling frequency; therefore, the frequencies can be entered in the formula in hertz, as long as the sampling frequency Ω_s is also in hertz):
  - (i) From equations (77)–(79), we have that

$$T_r = +\min\{(950-800), (1200-1050)\} = 150 \text{ Hz} \tag{81}$$

$$\Omega_{c_1} = 800+75 = 875 \text{ Hz} \tag{82}$$

$$\Omega_{c_2} = 1200-75 = 1125 \text{ Hz} \tag{83}$$

Example 5.4 - Solution

- (cont.)
  - (ii) From equations (69) and (70),

$$\delta_p = \frac{10^{0.05} - 1}{10^{0.05} + 1} = 0.0575 \quad (84)$$

$$\delta_r = 10^{-0.05 \times 45} = 0.005\,62 \quad (85)$$

$$(86)$$

  - (iii) $\delta = \min\{0.0575, 0.005\,62\} = 0.005\,62$
  - (iv) From equations (71) and (72),

$$A_p = 20 \log \frac{1 + 0.005\,62}{1 - 0.005\,62} = 0.0977 \text{ dB} \quad (87)$$

$$A_r = -20 \log 0.005\,62 = 45 \text{ dB} \quad (88)$$

Example 5.4 - Solution

- (cont.)
  - (v) Ω_r has already been computed as 150 Hz in step (i).
  - (vi) From equation (73), since $A_r = 45$ dB, then

$$\beta = 0.5842(45-21)^{0.4} + 0.078\,86(45-21) = 3.975\,4327 \tag{89}$$

  - (vii) From equation (74), since $A_r = 45$ dB, then

$$D = \frac{(45-7.95)}{14.36} = 2.580\,0835 \tag{90}$$

  - (viii) Since the sampling period is $T = \frac{1}{6000}$ s, we have, from equation (75),

$$M \geq \frac{6000 \times 2.580\,0835}{150} = 103.203\,34 \quad \Rightarrow \quad M = 104 \tag{91}$$

Example 5.4 - Solution

- This whole procedure is implemented by a simple MATLAB script:

```
Ap = 1; Ar = 45;
Omega_p1 = 800; Omega_r1 = 950;
Omega_r2 = 1050; Omega_p2 = 1200;
Omega_s = 6000;
delta_p = (10^(0.05*Ap) - 1)/(10^(0.05*Ap) + 1);
delta_r = 10^(-0.05*Ar);
F = [Omega_p1 Omega_r1 Omega_r2 Omega_p2];
A = [1 0 1];
ripples = [delta_p delta_r delta_p];
[M,Wn,beta,FILTYPE] =
kaiserord(F,A,ripples,Omega_s);
```

which yields as outputs `beta = 3.9754` and `M = 104`, as determined above.

Example 5.4 - Solution

- In this short script, the auxiliary vectors `A` and `ripples` specify the desired gain and allowed ripple, respectively, in each filter band.
- The Kaiser window coefficients are determined by:

```
kaiser_win = kaiser(M+1,beta);
```

  and are shown in Figure 12 along with the associated magnitude response.

Example 5.4 - Solution

(a)

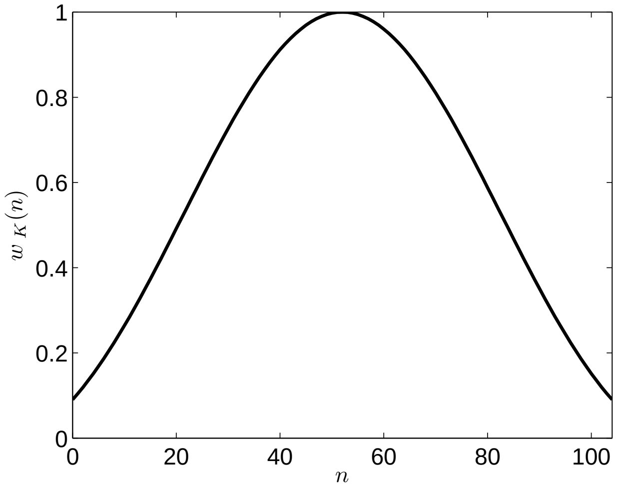

(b)

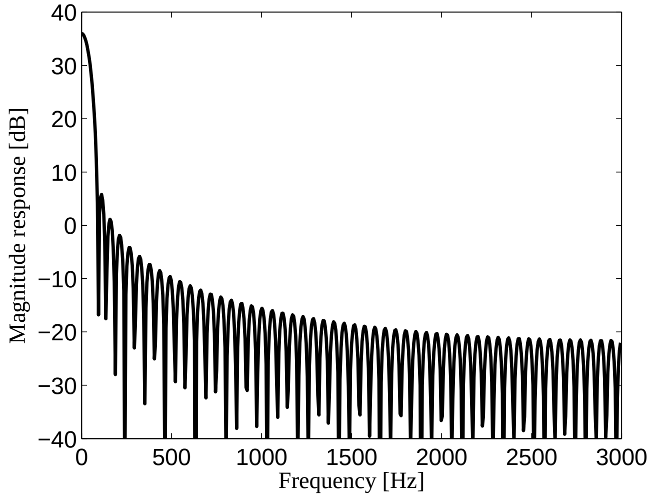

Figure 12: Kaiser window: (a) window function; (b) magnitude response.

Example 5.4 - Solution

- The desired filter is obtained using the `fir1` command, as exemplified by:

  `h = fir1(M,Wn,FILTYPE,kaiser_win,'noscale');`

  where the `noscale` flag avoids the unitary gain at the first passband center imposed by MATLAB.

- The designed filter characteristics are summarized in Table 9.

Example 5.4 - Solution

Table 9: Characteristics of the designed filter.

Ω_{c_1}	875 Hz
Ω_{c_2}	1125 Hz
Ω_{p_1}	800 Hz
Ω_{r_1}	950 Hz
Ω_{r_2}	1050 Hz
Ω_{p_2}	1200 Hz
δ_p	0.0575
δ_r	0.005 62
T_r	150 Hz
D	2.580 0835
β	3.975 4327
M	104

Example 5.4 - Solution

- The filter coefficients $h(n)$ are given in Table 10. Once again, due to the symmetry inherent to the Kaiser window function, Table 10 only shows half of the filter coefficients, as the remaining coefficients are obtained as $h(n) = h(M - n)$.
- The filter impulse response and associated magnitude response are shown in Figure 13.

Example 5.4 - Solution

Table 10: Filter coefficients using the Kaiser window.

$h(0)$ to $h(52)$			
$h(0) = 0.0003$	$h(14) = -0.0028$	$h(28) = 0.0000$	$h(42) = 0.0288$
$h(1) = 0.0005$	$h(15) = 0.0032$	$h(29) = -0.0013$	$h(43) = 0.0621$
$h(2) = 0.0002$	$h(16) = 0.0070$	$h(30) = 0.0027$	$h(44) = 0.0331$
$h(3) = -0.0001$	$h(17) = 0.0038$	$h(31) = 0.0087$	$h(45) = -0.0350$
$h(4) = -0.0000$	$h(18) = -0.0040$	$h(32) = 0.0061$	$h(46) = -0.0733$
$h(5) = 0.0001$	$h(19) = -0.0083$	$h(33) = -0.0081$	$h(47) = -0.0381$
$h(6) = -0.0003$	$h(20) = -0.0042$	$h(34) = -0.0203$	$h(48) = 0.0394$
$h(7) = -0.0011$	$h(21) = 0.0042$	$h(35) = -0.0123$	$h(49) = 0.0807$
$h(8) = -0.0008$	$h(22) = 0.0081$	$h(36) = 0.0146$	$h(50) = 0.0411$
$h(9) = 0.0011$	$h(23) = 0.0038$	$h(37) = 0.0339$	$h(51) = -0.0415$
$h(10) = 0.0028$	$h(24) = -0.0033$	$h(38) = 0.0194$	$h(52) = 0.9167$
$h(11) = 0.0018$	$h(25) = -0.0055$	$h(39) = -0.0218$	
$h(12) = -0.0021$	$h(26) = -0.0020$	$h(40) = -0.0484$	
$h(13) = -0.0050$	$h(27) = 0.0011$	$h(41) = -0.0266$	

Example 5.4 - Solution

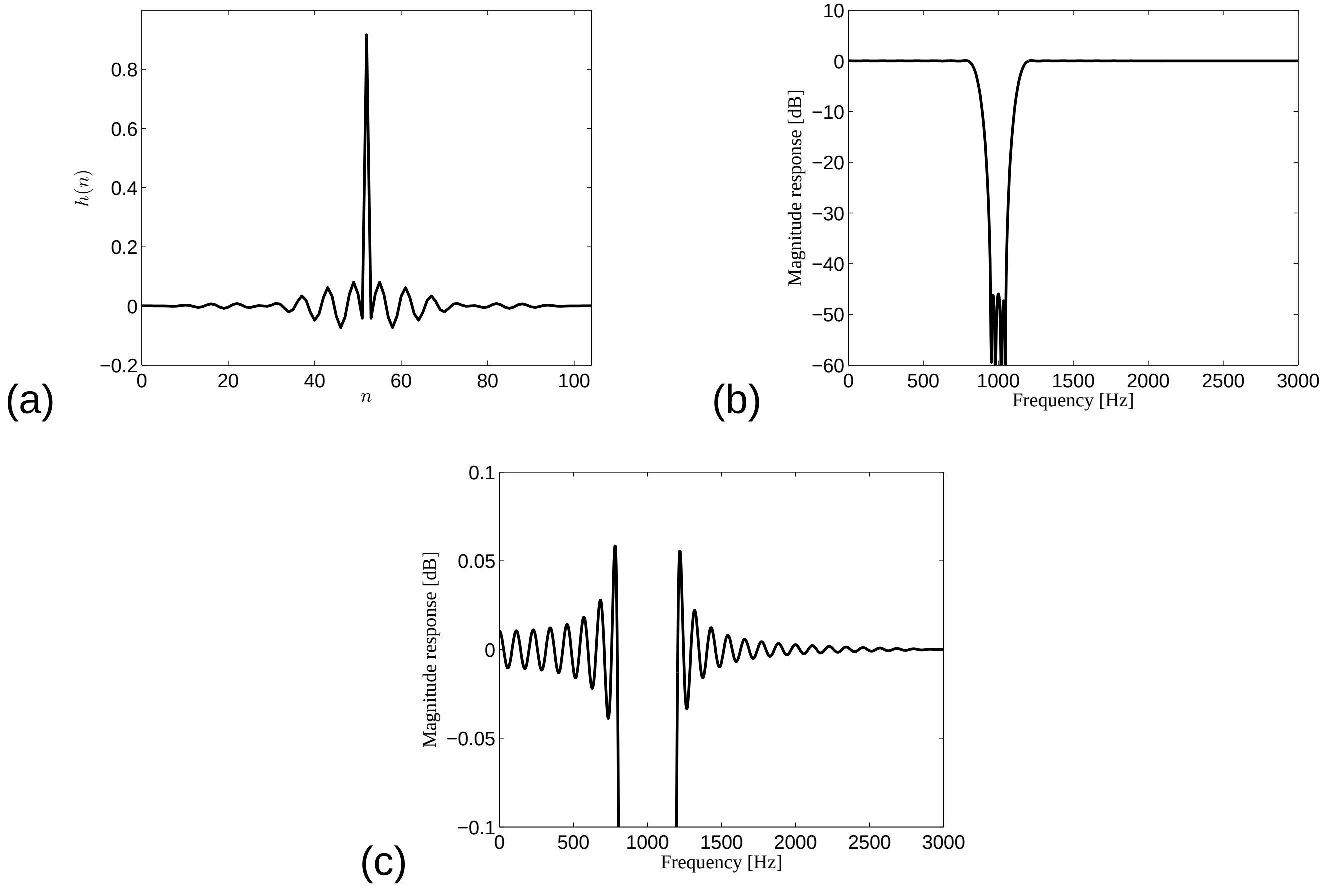

Figure 13: Resulting bandstop filter: (a) impulse response; (b) magnitude response; (c) passband detail.

Dolph-Chebyshev window

- Based on the Mth-order Chebyshev polynomial given by

$$C_M(x) = \begin{cases} \cos\left[M \cos^{-1}(x)\right], & \text{for } |x| \leq 1 \\ \cosh\left[M \cosh^{-1}(x)\right], & \text{for } |x| > 1 \end{cases} \quad (92)$$

the Dolph-Chebyshev window is defined as

$$w_{DC}(n) = \begin{cases} \frac{1}{M+1}\left\{\frac{1}{r} + 2\sum_{i=1}^{\frac{M}{2}} C_M\left[x_0 \cos\left(\frac{i\pi}{M+1}\right)\right]\cos\left(\frac{2ni\pi}{M+1}\right)\right\}, & \text{for } |n| \leq \frac{M}{2} \\ 0, & \text{for } |n| > \frac{M}{2} \end{cases} \quad (93)$$

where r is the ripple ratio defined as $r = \frac{\delta_r}{\delta_p}$ and

$$x_0 = \cosh\left[\frac{1}{M}\cosh^{-1}\left(\frac{1}{r}\right)\right] \quad (94)$$

Dolph-Chebyshev window

- The procedure for designing FIR filters using the Dolph-Chebyshev window is very similar to the one for the Kaiser window:
  - (i) Perform steps (i) and (ii) of the Kaiser procedure.
  - (ii) Determine $r = \frac{\delta_r}{\delta_p}$.
  - (iii) Perform steps (iii)–(v) and (vii)–(viii) of the Kaiser procedure, to determine the filter order M. In step (vii), however, as the stopband attenuation achieved with the Dolph-Chebyshev window is typically 1 to 4 dB higher than that obtained using the Kaiser window, one should compute D for the Dolph-Chebyshev window using equation (5.74) with A_r replaced by $A_r + 2.5$.
  - (iv) With r and M determined, compute x_0 from equation (94), and then compute the window coefficients from equation (93).
  - (v) We are now ready to form the sequence $h'(n) = w_{DC}(n)h(n)$, where $h(n)$ is the ideal filter impulse response computed in step (86).
  - (vi) Perform step (x) of the Kaiser procedure to determine the resulting FIR filter.

Dolph-Chebyshev window

- Overall, the Dolph-Chebyshev window is characterized by:
  - The main-lobe width, and consequently the resulting filter transition band, can be controlled by varying M.
  - The ripple ratio is controlled through an independent parameter r.
  - All secondary lobes have the same amplitude. Therefore, the stopband of the resulting filter is equiripple.

Maximally flat FIR filter approximation

- Maximally flat approximations should be employed when a signal must be preserved with minimal error around the zero frequency or when a monotone frequency response is necessary.

- FIR filters with a maximally flat frequency response at $\omega = 0$ and $\omega = \pi$ were introduced by Herrmann. We consider here, following the standard literature on the subject, the lowpass Type-I FIR filter of even order M and symmetric impulse response.

- In this case, the frequency response of a maximally flat FIR filter is determined in such a way that $H(e^{j\omega}) - 1$ has $2L$ zeros at $\omega = 0$, and $H(e^{j\omega})$ has $2K$ zeros at $\omega = \pi$.

- To achieve a maximally flat response, the filter order M must satisfy $M = (2K + 2L - 2)$. Thus, the first $2L - 1$ derivatives of $H(e^{j\omega})$ are zero at $\omega = 0$, and the first $2K - 1$ derivatives of $H(e^{j\omega})$ are zero at $\omega = \pi$.

Maximally flat FIR filter approximation

- If the above two conditions are satisfied, $H(e^{j\omega})$ can be written either as

$$\begin{aligned} H(e^{j\omega}) &= \left(\cos\frac{\omega}{2}\right)^{2K}\sum_{n=0}^{L-1} d(n)\left(\sin\frac{\omega}{2}\right)^{2n} \\ &= \left(\frac{1+\cos\omega}{2}\right)^{K}\sum_{n=0}^{L-1} d(n)\left(\frac{1-\cos\omega}{2}\right)^{n} \end{aligned} \tag{95}$$

- Or as

$$\begin{aligned} H(e^{j\omega}) &= 1-\left(\sin\frac{\omega}{2}\right)^{2L}\sum_{n=0}^{K-1} \hat{d}(n)\left(\cos\frac{\omega}{2}\right)^{2n} \\ &= 1-\left(\frac{1-\cos\omega}{2}\right)^{L}\sum_{n=0}^{K-1} \hat{d}(n)\left(\frac{1+\cos\omega}{2}\right)^{n} \end{aligned} \tag{96}$$

Maximally flat FIR filter approximation

- Where the coefficients $d(n)$ or $\hat{d}(n)$ are respectively given by

$$d(n) = \frac{(K-1+n)!}{(K-1)!n!} \tag{97}$$

$$\hat{d}(n) = \frac{(L-1+n)!}{(L-1)!n!} \tag{98}$$

- Note that from equations (95) and (97), $H(e^{j\omega})$ is real and positive.
- Therefore, for the maximally flat filters, $|H(e^{j\omega})| = H(e^{j\omega})$.
- From the above equations it is also easy to see that $H(e^{j\omega})$ can be expressed as a sum of complex exponentials in ω having frequencies ranging from $(-K-L+1)$ to $(K+L-1)$, with an increment of 1.

Maximally flat FIR filter approximation

- Therefore, from Theorem 5.1, one can see that $h(n)$ can be exactly recovered by sampling $H(e^{j\omega})$ at $(2K + 2L - 1) = M + 1$ equally spaced points located at frequencies $\omega = 2\pi n/(M + 1)$, for $n = 0, 1, \ldots, M$, and taking the IDFT, as in the frequency sampling approach.

- A more efficient implementation, however, results from writing the transfer function as

$$H(z) = \left(\frac{1 + z^{-1}}{2}\right)^{2K} \sum_{n=0}^{L-1} (-1)^n d(n) z^{-(L-1-n)} \left(\frac{1 - z^{-1}}{2}\right)^{2n} \tag{99}$$

or

$$H(z) = z^{-\frac{M}{2}} - (-1)^L \left(\frac{1 - z^{-1}}{2}\right)^{2L} \sum_{n=0}^{K-1} \hat{d}(n) z^{-(K-1-n)} \left(\frac{1 + z^{-1}}{2}\right)^{2n} \tag{100}$$

Maximally flat FIR filter approximation

- These equations require significantly fewer multipliers than the direct-form implementation.
- The drawback with these designs is the large dynamic range necessary to represent the sequences $d(n)$ and $\hat{d}(n)$.
- This can be avoided by an efficient cascade implementation of these coefficients utilizing the following relationships:

$$d(n+1) = d(n)\frac{K+n}{n+1} \tag{101}$$

$$\hat{d}(n+1) = \hat{d}(n)\frac{L+n}{n+1} \tag{102}$$

Maximally flat FIR filter approximation

- In the procedure described above, the sole design parameters for the maximally flat FIR filters are the values of K and L.

- Given a desired magnitude response, as depicted in Figure 14, the transition band is defined as the region where the magnitude response varies from 0.95 to 0.05, and the normalized center frequency is the center of this band ($\omega_c = \frac{\omega_p + \omega_r}{2}$).

- If the transition band in rad/sample is T_r, we need to compute the following parameters:

$$M_1 = \left(\frac{\pi}{T_r} \right)^2 \tag{103}$$

$$\rho = \frac{1 + \cos \omega_c}{2} \tag{104}$$

Maximally flat FIR filter approximation

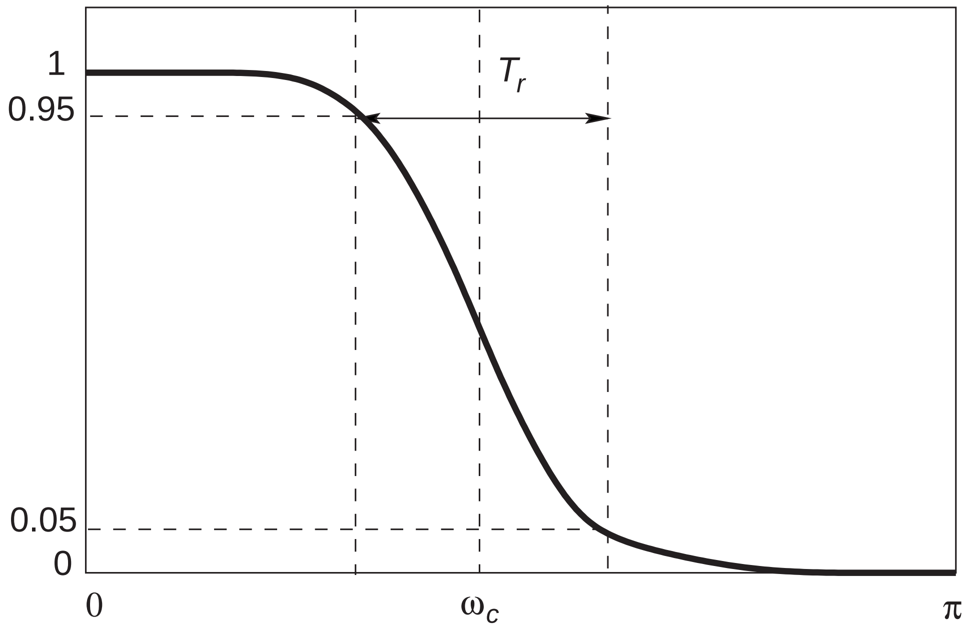

Figure 14: Typical specification of a maximally flat lowpass FIR filter.

Maximally flat FIR filter approximation

- Then, for all integer values of M_p in the range $M_1 \leq M_p \leq 2M_1$, we compute K_p as the nearest integer to ρM_p.
- We then choose K_p^* and M_p^* as the values of K_p and M_p for which the ratio $\frac{K_p}{M_p}$ is closest to ρ.
- The desired values of K, L, and M, are given by

$$K = K_p^* \tag{105}$$

$$L = M_p^* - K_p^* \tag{106}$$

$$M = 2K + 2L - 2 = 2M_p^* - 2 \tag{107}$$

Example 5.5

- Design a maximally flat lowpass filter satisfying the specification below:

$$\left.\begin{aligned} \Omega_c &= 0.3\pi \text{ rad/s} \\ T_r &= 0.2\pi \text{ rad/s} \\ \Omega_s &= 2\pi \text{ rad/s} \end{aligned}\right\} \tag{108}$$

Example 5.5 - Solution

- One may use the script:

```
Omega_c = 0.3*pi; Tr = 0.2*pi; Omega_s = 2*pi;
M1 = (pi/Tr)^2;
rho = (1 + cos(Omega_c))/2;
Mp = ceil(M1):floor(2*M1);
Kp = round(rho*Mp);
rho_p = Kp./Mp;
[value,index] = min(abs(rho_p - rho));
K = Kp(index); L = Mp(index)-Kp(index); M =
2*Mp(index)-2;
```

to obtain the values of $K = 27$, $L = 7$, and $M = 66$.

Example 5.5 - Solution

- The resulting coefficients $d(n)$, as given in equation (101), may be determined as

```
d(1) = 1;
for i = 0:L-2,
  d(i+2) = d(i+1)*(K+i)/(i+1);
end;
```

  and are seen in Table 11.

- Notice that in this case, even though the filter order is $M = 66$, there are only $L = 7$ nonzero coefficients $d(n)$.

Example 5.5 - Solution

Table 11: Coefficients of the lowpass filter designed with the maximally flat method.

$d(0)$ to $d(5)$
$d(0) = 1$
$d(1) = 27$
$d(2) = 378$
$d(3) = 3\,654$
$d(4) = 27\,405$
$d(5) = 169\,911$
$d(6) = 906\,192$

Example 5.5

- The corresponding magnitude response can be determined as:

```
omega = 2*pi.*(0:M)/(M+1);
i = (0:L-1)';
for k = 0:M,
   H(k+1) = d*sin(omega(k+1)/2).^(2*i);
end;
H = H.*cos(omega./2).^(2*K);
```

the result of which is depicted in Figure 15.

△

Example 5.5 - Solution

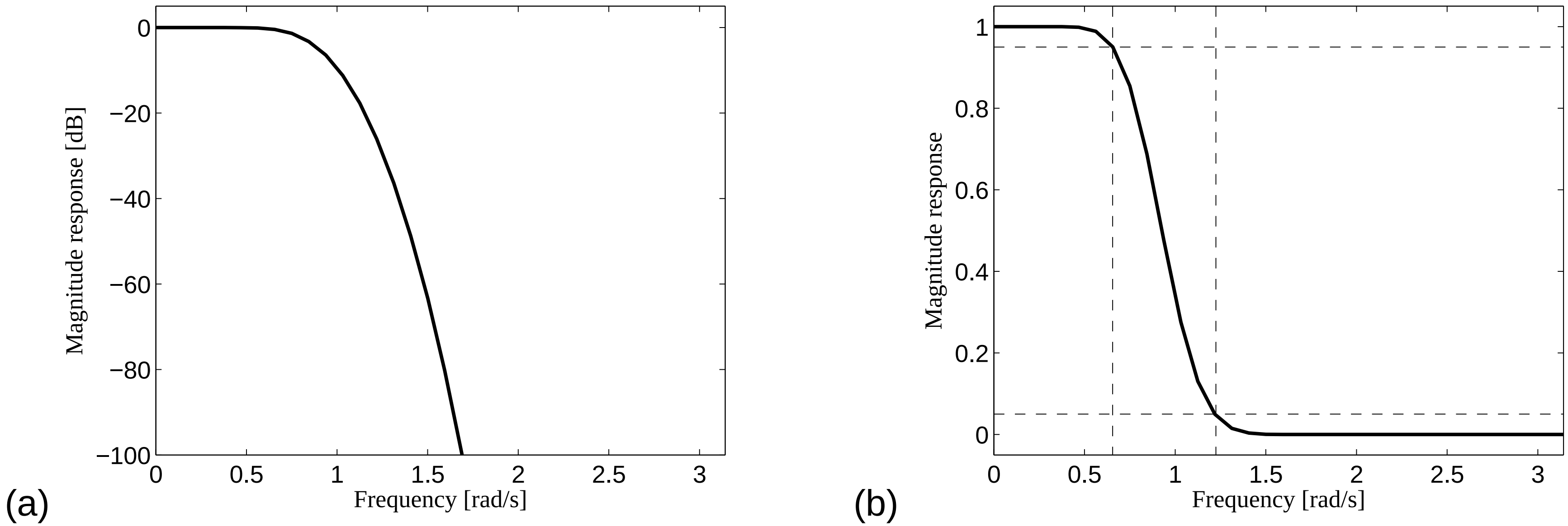

Figure 15: magnitude response of maximally flat lowpass FIR filter: (a) linear scale; (b) dB scale.

FIR filter approximation by optimization

- The window method seen in Section 5.4 has a very straightforward design procedure for approximating the desired magnitude response. However, the window method is not efficient for designing, for example, FIR filters with different ripples in the passband and stopband, or nonsymmetric bandpass or bandstop filters.
- To fill this gap, in this section we present several numerical algorithms for designing more general FIR digital filters.
- In many signal processing systems, filters with linear or zero phase are required. Unfortunately, filters designed to have zero phase are not causal; this can be a problem in applications where very little processing delay is permissible.
- Also, nonlinear phase causes distortion in the processed signal, which can be very perceptible in applications like data transmission, image processing, and so on.

FIR filter approximation by optimization

- One of the major advantages of using an FIR system instead of a causal IIR system is that FIR systems can be designed with exact linear phase.
- As seen in Subsection 4.2.3, there are four distinct cases where an FIR filter presents linear phase. To present general algorithms for designing linear-phase FIR filters, a unified representation of these four cases is necessary.
- We define an auxiliary function $P(\omega)$ as

$$P(\omega) = \sum_{l=0}^{L} p(l) \cos(\omega l) \tag{109}$$

where $L+1$ is the number of cosine functions in the expression of $H(e^{j\omega})$.

FIR filter approximation by optimization

- Based on this function, we can express the frequency response of the four types of linear-phase FIR filters as:
  - Type I: Even order M and symmetric impulse response. We get

$$\begin{aligned} H(e^{j\omega}) &= e^{-j\omega\frac{M}{2}} \sum_{m=0}^{\frac{M}{2}} a(m)\cos(\omega m) \\ &= e^{-j\omega\frac{M}{2}} \sum_{l=0}^{\frac{M}{2}} p(l)\cos(\omega l) \\ &= e^{-j\omega\frac{M}{2}} P(\omega) \end{aligned} \tag{110}$$

with

$$a(m) = p(m), \text{ for } m = 0, 1, \ldots, L \tag{111}$$

where $L = \frac{M}{2}$.

FIR filter approximation by optimization

- (cont.)
  - Type II: Odd order M and symmetric impulse response. In this case, we have

$$H(e^{j\omega}) = e^{-j\omega\frac{M}{2}} \sum_{m=1}^{\frac{M+1}{2}} b(m) \cos\left[\omega\left(m - \frac{1}{2}\right)\right] \tag{112}$$

Using

$$b(m) = \begin{cases} p(0) + \frac{1}{2}p(1), & \text{for } m = 1 \\ \frac{1}{2}\left(p(m-1) + p(m)\right), & \text{for } m = 2, 3, \ldots, L \\ \frac{1}{2}p(L), & \text{for } m = L+1 \end{cases} \tag{113}$$

FIR filter approximation by optimization

- With $L = \frac{M-1}{2}$, then $H(e^{j\omega})$ can be written in the form

$$H(e^{j\omega}) = e^{-j\omega\frac{M}{2}} \cos\left(\frac{\omega}{2}\right) P(\omega) \tag{114}$$

using the trigonometric identity

$$2\cos\left(\frac{\omega}{2}\right)\cos(\omega m) = \cos\left[\omega\left(m + \frac{1}{2}\right)\right] + \cos\left[\omega\left(m - \frac{1}{2}\right)\right] \tag{115}$$

- The complete algebraic development is left as an exercise to the interested reader.

FIR filter approximation by optimization

- (cont.)
  - Type III: Even order M and antisymmetric impulse response. In this case, we have

$$H(e^{j\omega}) = e^{-j(\omega\frac{M}{2}-\frac{\pi}{2})} \sum_{m=1}^{\frac{M}{2}} c(m)\sin(\omega m) \tag{116}$$

and then, by substituting

$$c(m) = \begin{cases} p(0) - \frac{1}{2}p(2), & \text{for } m = 1 \\ \frac{1}{2}\left(p(m-1) - p(m+1)\right), & \text{for } m = 2, 3, \ldots, (L-1) \\ \frac{1}{2}p(m-1), & \text{for } m = L, L+1 \end{cases} \tag{117}$$

FIR filter approximation by optimization

- With $L = \frac{M}{2} - 1$, equation (116) can be written as

$$H(e^{j\omega}) = e^{-j\left(\omega\frac{M}{2} - \frac{\pi}{2}\right)} \sin\omega P(\omega) \tag{118}$$

using, in this case, the identity

$$\sin\omega \cos(\omega m) = \sin[\omega(m+1)] - \sin[\omega(m-1)] \tag{119}$$

- Once again, the algebraic proof is left as an exercise at the end of this chapter.

FIR filter approximation by optimization

- (cont.)
  - Type IV: Odd order M and antisymmetric impulse response. We have that

$$H(e^{j\omega}) = e^{-j(\omega\frac{M}{2}-\frac{\pi}{2})}\sum_{m=1}^{\frac{M+1}{2}} d(m)\sin\left[\omega\left(m-\frac{1}{2}\right)\right] \tag{120}$$

By substituting

$$d(m) = \begin{cases} p(0)-\frac{1}{2}p(1), & \text{for } m=1 \\ \frac{1}{2}\left(p(m-1)-p(m)\right), & \text{for } m=2,3,\ldots,L \\ \frac{1}{2}p(L), & \text{for } m=L+1 \end{cases} \tag{121}$$

FIR filter approximation by optimization

- With $L = \frac{M-1}{2}$, then $H(e^{j\omega})$ can be written as

$$H(e^{j\omega}) = e^{-j\left(\omega \frac{M}{2} - \frac{\pi}{2}\right)} \sin\left(\frac{\omega}{2}\right) P(\omega) \tag{122}$$

using the identity

$$2\sin\left(\frac{\omega}{2}\right)\cos(\omega m) = \sin\left[\omega\left(m + \frac{1}{2}\right)\right] - \sin\left[\omega\left(m - \frac{1}{2}\right)\right] \tag{123}$$

FIR filter approximation by optimization

- Equations (110), (114), (118), and (122) indicate that we can write the frequency response for any linear-phase FIR filter as

$$H(e^{j\omega}) = e^{-j(\alpha\omega-\beta)}Q(\omega)P(\omega) = e^{-j(\alpha\omega-\beta)}A(\omega) \tag{124}$$

  where $A(\omega) = Q(\omega)P(\omega)$, $\alpha = \frac{M}{2}$, and for each case we have that:
  - Type I: $\beta = 0$ and $Q(\omega) = 1$
  - Type II: $\beta = 0$ and $Q(\omega) = \cos(\frac{\omega}{2})$
  - Type III: $\beta = \frac{\pi}{2}$ and $Q(\omega) = \sin(\omega)$
  - Type IV: $\beta = \frac{\pi}{2}$ and $Q(\omega) = \sin(\frac{\omega}{2})$.

FIR filter approximation by optimization

- Let $D(\omega)$ be the desired amplitude response. We define the weighted error function as

$$E(\omega) = W(\omega)(D(\omega) - A(\omega)) \tag{125}$$

- We can then write $E(\omega)$ as

$$\begin{aligned} E(\omega) &= W(\omega)(D(\omega) - Q(\omega)P(\omega)) \\ &= W(\omega)Q(\omega)\left(\frac{D(\omega)}{Q(\omega)} - P(\omega)\right) \end{aligned} \tag{126}$$

for all $0 \leq \omega \leq \pi$, as $Q(\omega)$ is independent of the coefficients for each ω.

FIR filter approximation by optimization

- Defining

$$W_q(\omega) = W(\omega)Q(\omega) \tag{127}$$

$$D_q(\omega) = \frac{D(\omega)}{Q(\omega)} \tag{128}$$

the error function can be rewritten as

$$E(\omega) = W_q(\omega)(D_q(\omega) - P(\omega)) \tag{129}$$

and one can formulate the optimization problem for approximating linear-phase FIR filters as:

- *Determine the set of coefficients* $p(l)$ *that minimizes some objective function of the weighted error* $E(\omega)$ *over a set of prescribed frequency bands.*

FIR filter approximation by optimization

- To solve such a problem numerically, we evaluate the weighted error function on a dense frequency grid with $0 \leq \omega_i \leq \pi$, for $i = 1, 2, \ldots, KM$, where M is the filter order, obtaining a good discrete approximation of $E(\omega)$.
- For most practical purposes, using $8 \leq K \leq 16$ is recommended. Points associated with the transition bands can be disregarded, and the remaining frequencies should be linearly redistributed in the passbands and stopbands to include their corresponding edges.

CAMBRIDGE UNIVERSITY PRESS

FIR filter approximation by optimization

- Thus, the following equation results

$$\mathbf{e} = \mathbf{W}_q \left(\mathbf{d}_q - \mathbf{U}\mathbf{p}\right) \tag{130}$$

where

$$\mathbf{e} = \left[E(\omega_1)\; E(\omega_2)\; \cdots \; E(\omega_{\overline{KM}})\right]^T \tag{131}$$

$$\mathbf{W}_q = \text{diag}\left[W_q(\omega_1)\; W_q(\omega_2)\; \cdots \; W_q(\omega_{\overline{KM}})\right] \tag{132}$$

$$\mathbf{d}_q = \left[D_q(\omega_1)\; D_q(\omega_2)\; \cdots \; D_q(\omega_{\overline{KM}})\right]^T \tag{133}$$

$$\mathbf{U} = \begin{bmatrix} 1 & \cos(\omega_1) & \cos(2\omega_1) & \ldots & \cos(L\omega_1) \\ 1 & \cos(\omega_2) & \cos(2\omega_2) & \ldots & \cos(L\omega_2) \\ \vdots & \vdots & \vdots & \ddots & \vdots \\ 1 & \cos(\omega_{\overline{KM}}) & \cos(2\omega_{\overline{KM}}) & \ldots & \cos(L\omega_{\overline{KM}}) \end{bmatrix} \tag{134}$$

$$\mathbf{p} = [p(0)\; p(1)\; \cdots \; p(L)]^T \tag{135}$$

FIR filter approximation by optimization

- With $\overline{KM} \leq KM$, as the original frequencies in the transition band were discarded.
- For the four standard types of filters, namely lowpass, highpass, bandpass, and bandstop, as well as differentiators and Hilbert transformers, the definitions of $W(\omega)$ and $D(\omega)$ are summarized in Table 12.

FIR filter approximation by optimization

Table 12: Weight functions and ideal magnitude responses for basic lowpass, highpass, bandpass, and bandstop filters, as well as differentiators and Hilbert transformers.

Filter type	Weight function $W(\omega)$	Ideal amplitude response $D(\omega)$
Lowpass	$\begin{cases} 1, & \text{for } 0 \leq \omega \leq \omega_p \\ \dfrac{\delta_p}{\delta_r}, & \text{for } \omega_r \leq \omega \leq \pi \end{cases}$	$\begin{cases} 1, & \text{for } 0 \leq \omega \leq \omega_p \\ 0, & \text{for } \omega_r \leq \omega \leq \pi \end{cases}$
Highpass	$\begin{cases} \dfrac{\delta_p}{\delta_r}, & \text{for } 0 \leq \omega \leq \omega_r \\ 1, & \text{for } \omega_p \leq \omega \leq \pi \end{cases}$	$\begin{cases} 0, & \text{for } 0 \leq \omega \leq \omega_r \\ 1, & \text{for } \omega_p \leq \omega \leq \pi \end{cases}$

FIR filter approximation by optimization

Filter type	Weight function $W(\omega)$	Ideal amplitude response $D(\omega)$
Bandpass	$\begin{cases} \dfrac{\delta_p}{\delta_r}, & \text{for } 0 \le \omega \le \omega_{r_1} \\ 1, & \text{for } \omega_{p_1} \le \omega \le \omega_{p_2} \\ \dfrac{\delta_p}{\delta_r}, & \text{for } \omega_{r_2} \le \omega \le \pi \end{cases}$	$\begin{cases} 0, & \text{for } 0 \le \omega \le \omega_{r_1} \\ 1, & \text{for } \omega_{p_1} \le \omega \le \omega_{p_2} \\ 0, & \text{for } \omega_{r_2} \le \omega \le \pi \end{cases}$
Bandstop	$\begin{cases} 1, & \text{for } 0 \le \omega \le \omega_{p_1} \\ \dfrac{\delta_p}{\delta_r}, & \text{for } \omega_{r_1} \le \omega \le \omega_{r_2} \\ 1, & \text{for } \omega_{p_2} \le \omega \le \pi \end{cases}$	$\begin{cases} 1, & \text{for } 0 \le \omega \le \omega_{p_1} \\ 0, & \text{for } \omega_{r_1} \le \omega \le \omega_{r_2} \\ 1, & \text{for } \omega_{p_2} \le \omega \le \pi \end{cases}$

FIR filter approximation by optimization

Filter type	Weight function $W(\omega)$	Ideal amplitude response $D(\omega)$
Differentiator	$\begin{cases} \dfrac{1}{\omega}, & \text{for } 0 < \omega \leq \omega_p \\ 0, & \text{for } \omega_p < \omega \leq \pi \end{cases}$	$\omega, \quad \text{for } 0 \leq \omega \leq \pi$
Hilbert transformer	$\begin{cases} 0, & \text{for } 0 \leq \omega < \omega_{p_1} \\ 1, & \text{for } \omega_{p_1} \leq \omega \leq \omega_{p_2} \\ 0, & \text{for } \omega_{p_2} < \omega \leq \pi \end{cases}$	$1, \quad \text{for } 0 \leq \omega \leq \pi$

FIR filter approximation by optimization

- It is important to remember all design constraints, due to the magnitude and phase characteristics of the four linear-phase filter types, as summarized below, where a ‘Yes’ entry indicates that the corresponding filter structure is suitable to implement the given filter type.

Filter type	Type I	Type II	Type III	Type IV
Lowpass	Yes	Yes	No	No
Highpass	Yes	No	No	Yes
Bandpass	Yes	Yes	Yes	Yes
Bandstop	Yes	No	No	No
Differentiator	No	No	Yes	Yes
Hilbert transformer	No	No	Yes	Yes

Weighted-least-squares method

- In the weighted-least-squares (WLS) approach, the idea is to minimize the square of the energy of the error function $E(\omega)$, that is

$$\min_{\mathbf{p}} \left\{ \|E(\omega)\|_2^2 \right\} = \min_{\mathbf{p}} \left\{ \int_0^{\pi} |E(\omega)|^2 \, d\omega \right\} \tag{136}$$

- For a discrete set of frequencies, this objective function is approximated by (see equations (130)–(135))

$$\|E(\omega)\|_2^2 \approx \frac{1}{\overline{\overline{KM}}} \sum_{k=1}^{\overline{KM}} |E(\omega_k)|^2 = \frac{1}{\overline{\overline{KM}}} \mathbf{e}^{\mathsf{T}} \mathbf{e} \tag{137}$$

since in these equations $\mathbf{e}$ is a real vector.

Weighted-least-squares method

- Using equation (130), and noting that $\mathbf{W}_{\mathrm{q}}$ is diagonal, we can write that

$$\begin{aligned}
\mathbf{e}^{\mathsf{T}}\mathbf{e} &= (\mathbf{d}_{\mathrm{q}}^{\mathsf{T}} - \mathbf{p}^{\mathsf{T}}\mathbf{U}^{\mathsf{T}})\mathbf{W}_{\mathrm{q}}^{\mathsf{T}}\mathbf{W}_{\mathrm{q}}(\mathbf{d}_{\mathrm{q}} - \mathbf{U}\mathbf{p}) \\
&= (\mathbf{d}_{\mathrm{q}}^{\mathsf{T}} - \mathbf{p}^{\mathsf{T}}\mathbf{U}^{\mathsf{T}})\mathbf{W}_{\mathrm{q}}^{2}(\mathbf{d}_{\mathrm{q}} - \mathbf{U}\mathbf{p}) \\
&= \mathbf{d}_{\mathrm{q}}^{\mathsf{T}}\mathbf{W}_{\mathrm{q}}^{2}\mathbf{d}_{\mathrm{q}} - \mathbf{d}_{\mathrm{q}}^{\mathsf{T}}\mathbf{W}_{\mathrm{q}}^{2}\mathbf{U}\mathbf{p} - \mathbf{p}^{\mathsf{T}}\mathbf{U}^{\mathsf{T}}\mathbf{W}_{\mathrm{q}}^{2}\mathbf{d}_{\mathrm{q}} + \mathbf{p}^{\mathsf{T}}\mathbf{U}^{\mathsf{T}}\mathbf{W}_{\mathrm{q}}^{2}\mathbf{U}\mathbf{p} \\
&= \mathbf{d}_{\mathrm{q}}^{\mathsf{T}}\mathbf{W}_{\mathrm{q}}^{2}\mathbf{d}_{\mathrm{q}} - 2\mathbf{p}^{\mathsf{T}}\mathbf{U}^{\mathsf{T}}\mathbf{W}_{\mathrm{q}}^{2}\mathbf{d}_{\mathrm{q}} + \mathbf{p}^{\mathsf{T}}\mathbf{U}^{\mathsf{T}}\mathbf{W}_{\mathrm{q}}^{2}\mathbf{U}\mathbf{p} \qquad (138)
\end{aligned}$$

  because $\mathbf{d}_{\mathrm{q}}^{\mathsf{T}}\mathbf{W}_{\mathrm{q}}^{2}\mathbf{U}\mathbf{p} = \mathbf{p}^{\mathsf{T}}\mathbf{U}^{\mathsf{T}}\mathbf{W}_{\mathrm{q}}^{2}\mathbf{d}_{\mathrm{q}}$, since these two terms are scalar.

- The minimization of such a functional is achieved by calculating its gradient vector with respect to the coefficient vector and equating it to zero.

Weighted-least-squares method

- Since

$$\nabla_{\mathbf{x}}\{\mathbf{A}\mathbf{x}\} = \mathbf{A}^{\mathsf{T}} \tag{139}$$

$$\nabla_{\mathbf{x}}\{\mathbf{x}^{\mathsf{T}}\mathbf{A}\mathbf{x}\} = (\mathbf{A} + \mathbf{A}^{\mathsf{T}})\mathbf{x} \tag{140}$$

this yields

$$\nabla_{\mathbf{p}}\left\{\mathbf{e}^{\mathsf{T}}\mathbf{e}\right\} = -2\mathbf{U}^{\mathsf{T}}\mathbf{W}_{\mathrm{q}}^{2}\mathbf{d}_{\mathrm{q}} + 2\mathbf{U}^{\mathsf{T}}\mathbf{W}_{\mathrm{q}}^{2}\mathbf{U}\mathbf{p}^{*} = \mathbf{0} \tag{141}$$

which implies that

$$\mathbf{p}^{*} = \left(\mathbf{U}^{\mathsf{T}}\mathbf{W}_{\mathrm{q}}^{2}\mathbf{U}\right)^{-1}\mathbf{U}^{\mathsf{T}}\mathbf{W}_{\mathrm{q}}^{2}\mathbf{d}_{\mathrm{q}} \tag{142}$$

- It can be shown that when the weight function $W(\omega)$ is made constant, the WLS approach is equivalent to the rectangular window presented in the previous section, and so suffers from the same problem of Gibbs' oscillations near the band edges.

- When $W(\omega)$ is not constant, the oscillations still occur but their energies will vary from band to band.

Weighted-least-squares method

- Amongst the several extensions and generalizations of the WLS approach, we refer here to the constrained-WLS and eigenfilter methods.
- In the constrained-WLS method, the designer specifies the maximum and minimum values allowed for the desired magnitude response in each band.
- In the proposed algorithm, the transition bands are not completely specified, as only their central frequencies need to be provided. The transition bands are then automatically adjusted to satisfy the constraints.
- The overall method consists of an iterative procedure where in each step a modified WLS design is performed, using Lagrange multipliers, and the constraints are subsequently tested and updated.

Weighted-least-squares method

- Such a procedure involves verification of the Kuhn-Tucker conditions, that is, it checks if all the resulting multipliers are non-negative, followed by a search routine that finds the positions of all local extremals in each band and tests if all the constraints are satisfied.
- For the eigenfilter method, the objective function in equation (129) is rewritten in a distinct form, and results from linear algebra are used to find the optimal filter for the resulting equation.
- With such a procedure, the eigenfilter method enables linear-phase FIR filters with different characteristics to be designed, and the WLS scheme appears as a special case of the eigenfilter approach.

Example 5.6

- Design a Hilbert transformer of order $M = 5$ using the WLS approach by choosing an appropriate grid of only 3 frequencies. Obtain $\mathbf{p}^*$ and the filter transfer function.

Example 5.6 - Solution

- For the odd order $M = 5$, the FIR Hilbert transformer should be of Type IV and the number of coefficients of **p** is $(L + 1)$, where $L = \frac{M-1}{2} = 2$.
- According to equations (129) and (130), the response error is

$$\mathbf{e} = \begin{bmatrix} \sin(\frac{\omega_1}{2}) & 0 & 0 \\ 0 & \sin(\frac{\omega_2}{2}) & 0 \\ 0 & 0 & \sin(\frac{\omega_3}{2}) \end{bmatrix} \left\{ \begin{bmatrix} \frac{1}{\sin(\frac{\omega_1}{2})} \\ \frac{1}{\sin(\frac{\omega_2}{2})} \\ \frac{1}{\sin(\frac{\omega_3}{2})} \end{bmatrix} - \begin{bmatrix} 1 & \cos\omega_1 & \cos 2\omega_1 \\ 1 & \cos\omega_2 & \cos 2\omega_2 \\ 1 & \cos\omega_3 & \cos 2\omega_3 \end{bmatrix} \begin{bmatrix} p(0) \\ p(1) \\ p(2) \end{bmatrix} \right\} \tag{143}$$

Example 5.6 - Solution

- We then form the frequency grid within the range defined in Table 12, such as

$$\left.\begin{aligned} \omega_1 &= \frac{\pi}{3} \\ \omega_2 &= \frac{\pi}{2} \\ \omega_2 &= \frac{2\pi}{3} \end{aligned}\right\} \tag{144}$$

in such a way that the error vector becomes

$$\mathbf{e} = \left\{ \begin{bmatrix} 1 \\ 1 \\ 1 \end{bmatrix} - \begin{bmatrix} \frac{1}{2} & 0 & 0 \\ 0 & \frac{\sqrt{2}}{2} & 0 \\ 0 & 0 & \frac{\sqrt{3}}{2} \end{bmatrix} \begin{bmatrix} 1 & \frac{1}{2} & -\frac{1}{2} \\ 1 & 0 & -1 \\ 1 & -\frac{1}{2} & -\frac{1}{2} \end{bmatrix} \begin{bmatrix} p(0) \\ p(1) \\ p(2) \end{bmatrix} \right\} \tag{145}$$

Example 5.6 - Solution

- The WLS solution requires the following matrix:

$$\mathbf{U}^{\mathsf{T}}\mathbf{W}_{q}^{2}\mathbf{U} = \frac{1}{4}\begin{bmatrix} 1 & 1 & 1 \\ \frac{1}{2} & 0 & -\frac{1}{2} \\ -\frac{1}{2} & -1 & -\frac{1}{2} \end{bmatrix}\begin{bmatrix} 1 & 0 & 0 \\ 0 & 2 & 0 \\ 0 & 0 & 3 \end{bmatrix}\begin{bmatrix} 1 & \frac{1}{2} & -\frac{1}{2} \\ 1 & 0 & -1 \\ 1 & -\frac{1}{2} & -\frac{1}{2} \end{bmatrix}$$

$$= \frac{1}{4}\begin{bmatrix} 6 & -1 & -4 \\ -1 & 1 & \frac{1}{2} \\ -4 & \frac{1}{2} & 3 \end{bmatrix} \tag{146}$$

whose inverse is

$$\left(\mathbf{U}^{\mathsf{T}}\mathbf{W}_{q}^{2}\mathbf{U}\right)^{-1} = \frac{1}{3}\begin{bmatrix} 22 & 8 & 28 \\ 8 & 16 & 8 \\ 28 & 8 & 40 \end{bmatrix} \tag{147}$$

Example 5.6 - Solution

- Then, the vector $\mathbf{p}^*$ is computed as follows

$$\begin{aligned}
\mathbf{p}^* &= \left(\mathbf{U}^{\mathsf{T}}\mathbf{W}_{\mathrm{q}}^2\mathbf{U}\right)^{-1}\mathbf{U}^{\mathsf{T}}\mathbf{W}_{\mathrm{q}}^2\mathbf{d}_{\mathrm{q}} \\
&= \frac{1}{3}\begin{bmatrix} 22 & 8 & 28 \\ 8 & 16 & 8 \\ 28 & 8 & 40 \end{bmatrix}\begin{bmatrix} 1 & 1 & 1 \\ \frac{1}{2} & 0 & -\frac{1}{2} \\ -\frac{1}{2} & -1 & -\frac{1}{2} \end{bmatrix}\begin{bmatrix} \frac{1}{2} & 0 & 0 \\ 0 & \frac{\sqrt{2}}{2} & 0 \\ 0 & 0 & \frac{\sqrt{3}}{2} \end{bmatrix}^2\begin{bmatrix} 2 & 0 & 0 \\ 0 & \sqrt{2} & 0 \\ 0 & 0 & \frac{2}{\sqrt{3}} \end{bmatrix}\begin{bmatrix} 1 \\ 1 \\ 1 \end{bmatrix} \\
&= \begin{bmatrix} 1.7405 \\ 0.8453 \\ 0.3263 \end{bmatrix} \qquad (148)
\end{aligned}$$

Example 5.6 - Solution

- According to equations (121), we then have

$$\left.\begin{aligned} d(1) &= p(0) - \tfrac{1}{2}p(1) = 2h(2) = 1.31785 \\ d(2) &= \tfrac{1}{2}(p(1) - p(2)) = 2h(1) = 0.2595 \\ d(3) &= \tfrac{1}{2}p(2) = 2h(0) = 0.16315 \end{aligned}\right\} \tag{149}$$

and the overall transfer function is given by

$$H(z) = 0.0816 + 0.1298z^{-1} + 0.6589z^{-2} - 0.6589z^{-3} - 0.1298z^{-4} - 0.0816z^{-5} \tag{150}$$

Example 5.6 - Solution

- If a Hilbert filter of same order is designed with the MATLAB `firls` command, which uses a uniform sampling to determine the frequency grid, the resulting transfer function is

$$\overline{\mathrm{H}}(z) = -0.0828 - 0.1853z^{-1} - 0.6277z^{-2} + 0.6277z^{-3} + 0.1853z^{-4} + 0.0828z^{-5} \tag{151}$$

- As can be observed in Figure 16, $\mathrm{H}(z)$ and $\overline{\mathrm{H}}(z)$ have very similar magnitude responses, with the differences arising from the nonuniform frequency grid employed in the $\mathrm{H}(z)$ design for didactic purposes.

Example 5.6 - Solution

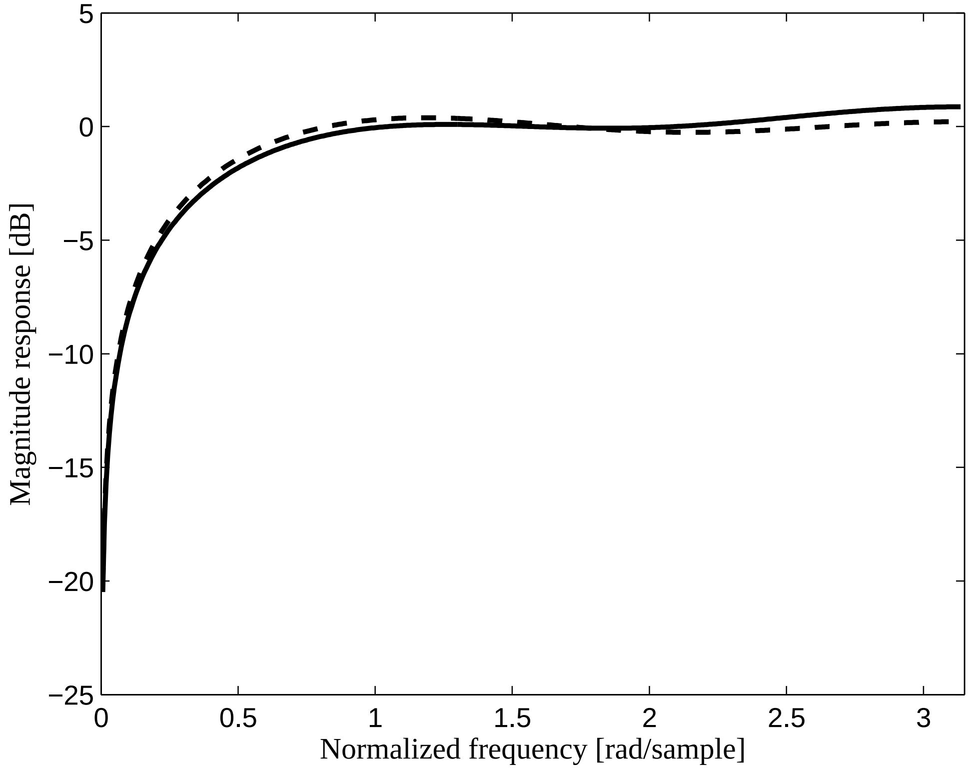

Figure 16: Magnitude responses of Hilbert transformers in Example 5.6: step-by-step $\mathrm{H}(z)$ design (solid line) and MATLAB $\overline{\mathrm{H}}(z)$ design (dashed line).

Chebyshev method

- In the Chebyshev optimization design approach, the idea is to minimize the maximum absolute value of the error function $E(\omega)$.

- Mathematically, such scheme is described by

$$\min_{\mathbf{p}}\{\|E(\omega)\|_{\infty}\} = \min_{\mathbf{p}}\left\{\max_{\omega\in F}\{|E(\omega)|\}\right\} \tag{152}$$

where F is the set of prescribed frequency bands. This problem can be solved with the help of the following important theorem:

Chebyshev method

- **Theorem (Alternation Theorem):** If $P(\omega)$ is a linear combination of $(L+1)$ cosine functions, that is

$$P(\omega) = \sum_{l=0}^{L} p(l) \cos(\omega l) \tag{153}$$

the necessary and sufficient condition for $P(\omega)$ to be the Chebyshev approximation of a continuous function $D(\omega)$ in F, a compact subset of $[0, \pi]$, is that the error function $E(\omega)$ must present at least $(L+2)$ extreme frequencies in F.

- That is, there must be at least $(L+2)$ points ω_k in F, where $\omega_0 < \omega_1 < \cdots < \omega_{L+1}$, such that

$$E(\omega_k) = -E(\omega_{k+1}), \text{ for } k = 0, 1, \ldots, L \tag{154}$$

and

$$|E(\omega_k)| = \max_{\omega \in F}\{|E(\omega)|\}, \text{ for } k = 0, 1, \ldots, (L+1) \tag{155}$$

Chebyshev method

- A proof of this theorem can be found in (Cheney, 1966).
- The extremes of $E(\omega)$ are related to the extremes of $A(\omega)$ defined in equation (125).
- The values of ω for which $\frac{\partial A(\omega)}{\partial \omega} = 0$ allow us to determine that the number N_k of extremes of $A(\omega)$ is such that:
  - Type I: $N_k \leq \frac{M+2}{2}$
  - Type II: $N_k \leq \frac{M+1}{2}$
  - Type III: $N_k \leq \frac{M}{2}$
  - Type IV: $N_k \leq \frac{M+1}{2}$

Chebyshev method

- In general, the extremes of $A(\omega)$ are also extremes of $E(\omega)$. However, $E(\omega)$ presents more extremes than $A(\omega)$, as $E(\omega)$ may present extremes at the band edges, which are, in general, not extremes of $A(\omega)$.

- The only exception to this rule occurs at the band edges $\omega = 0$ or $\omega = \pi$, where $A(\omega)$ also presents an extreme.

- For instance, for a Type-I bandstop filter, as depicted in Figure 17, $E(\omega)$ will have up to $(\frac{M}{2} + 5)$ extremes, where $(\frac{M}{2} + 1)$ are extremes of $A(\omega)$, and the other four are band edges.

Chebyshev method

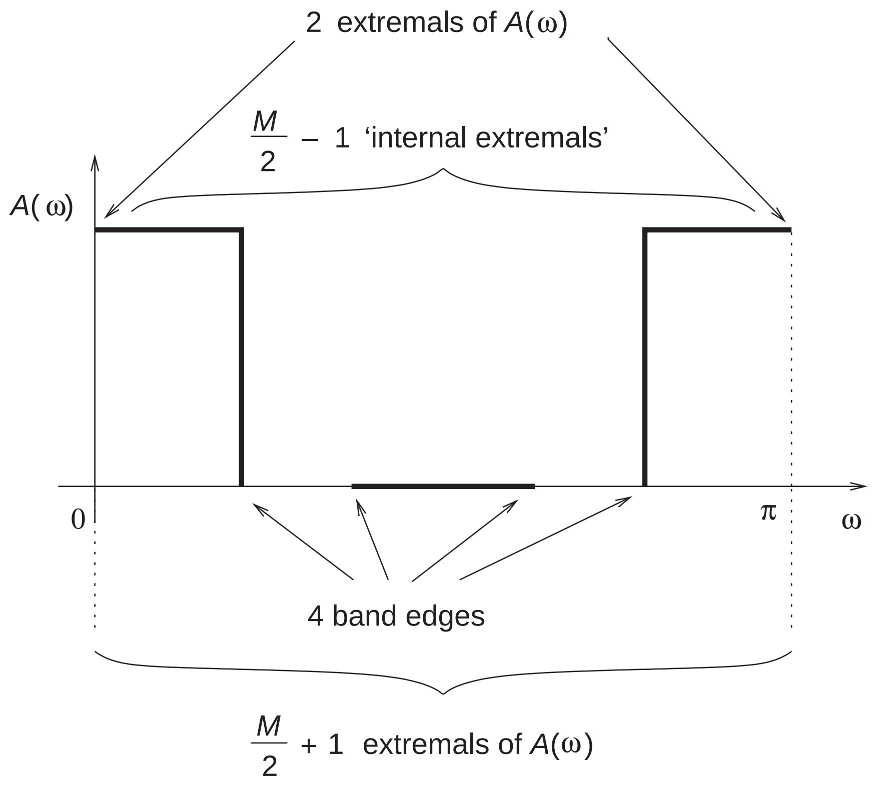

Figure 17: Extremes of $A(\omega)$ for a bandstop filter.

Chebyshev method

- To solve the Chebyshev approximation problem, we briefly describe the Remez exchange algorithm that searches for the extreme frequencies of $E(\omega)$ through the following steps:
  - (i) Initialize an estimate for the extreme frequencies $\omega_0, \omega_1, \ldots, \omega_{L+1}$ by selecting $(L+2)$ equally spaced frequencies at the bands specified for the desired filter.

Chebyshev method

- (cont.)
  - (ii) Find $P(\omega_k)$ and δ such that

$$W_q(\omega_k)(D_q(\omega_k) - P(\omega_k)) = (-1)^k\delta, \text{ for } k = 0, 1, \ldots, (L+1) \quad (156)$$

This equation can be written in a matrix form and have its solution analytically calculated. Such a procedure, however, is computationally intensive. An alternative and more efficient approach computes δ by

$$\delta = \frac{a_0 D_q(\omega_0) + a_1 D_q(\omega_1) + \cdots + a_{L+1} D_q(\omega_{L+1})}{\frac{a_0}{W_q(\omega_0)} - \frac{a_1}{W_q(\omega_1)} + \cdots + \frac{(-1)^{L+1} a_{L+1}}{W_q(\omega_{L+1})}} \quad (157)$$

where

$$a_k = \prod_{i=0, i\neq k}^{L+1} \frac{1}{\cos\omega_k - \cos\omega_i} \quad (158)$$

Chebyshev method

- (cont.)
  - (iii) Use the barycentric-form Lagrange interpolator for $P(\omega)$, that is

$$P(\omega) = \begin{cases} c_k, & \text{for } \omega = \omega_k \in \{\omega_0, \omega_1, \ldots, \omega_L\} \\ \dfrac{\displaystyle\sum_{i=0}^{L} \frac{\beta_i}{\cos\omega - \cos\omega_i} c_i}{\displaystyle\sum_{i=0}^{L} \frac{\beta_i}{\cos\omega - \cos\omega_i}}, & \text{for } \omega \notin \{\omega_0, \omega_1, \ldots, \omega_L\} \end{cases} \tag{159}$$

where, for $k = 0, 1, \ldots, (L+1)$:

$$c_k = D_q(\omega_k) - (-1)^k \frac{\delta}{W_q(\omega_k)} \tag{160}$$

$$\beta_k = \prod_{i=0, i\neq k}^{L} \frac{1}{\cos\omega_k - \cos\omega_i} = a_k(\cos\omega_k - \cos\omega_{L+1}) \tag{161}$$

Chebyshev method

- (cont.)
  - (iv) Evaluate $|E(\omega)|$ in a dense set of frequencies. If $|E(\omega)| \leq |\delta|$ for all frequencies in the set, the optimal solution has been found, go to the next step. If $|E(\omega)| > |\delta|$ for some frequencies, a new set of candidate extremes must be chosen as the peaks of $|E(\omega)|$. In that manner, we force δ to grow and to converge to its upper limit. If there are more than $(L+2)$ peaks in $|E(\omega)|$, keep the locations of the $(L+2)$ largest values of the peaks of $|E(\omega)|$, making sure that the band edges are always kept, and return to step (ii).

Chebyshev method

- (cont.)
  - (v) Since $P(\omega)$ is a sum of $(L+1)$ cosines, with frequencies from zero to L, then it is also a sum of $(2L+1)$ complex exponentials, with frequencies from $-L$ to L. Then, from Theorem 4.1, $p(l)$ can be exactly recovered by sampling $P(\omega)$ at $(2L+1)$ equally spaced frequencies $\omega = \frac{2\pi n}{2L+1}$, for $n = 0, 1, \ldots, 2L$ and taking the inverse DFT. The resulting impulse response follows from equations (111), (113), (117), or (121), depending on the filter type.
- The corresponding MATLAB function for such an algorithm is `firpm` (see Section 5.8).

Example 5.7

- Design the PCM filter specified as in Figure 18.

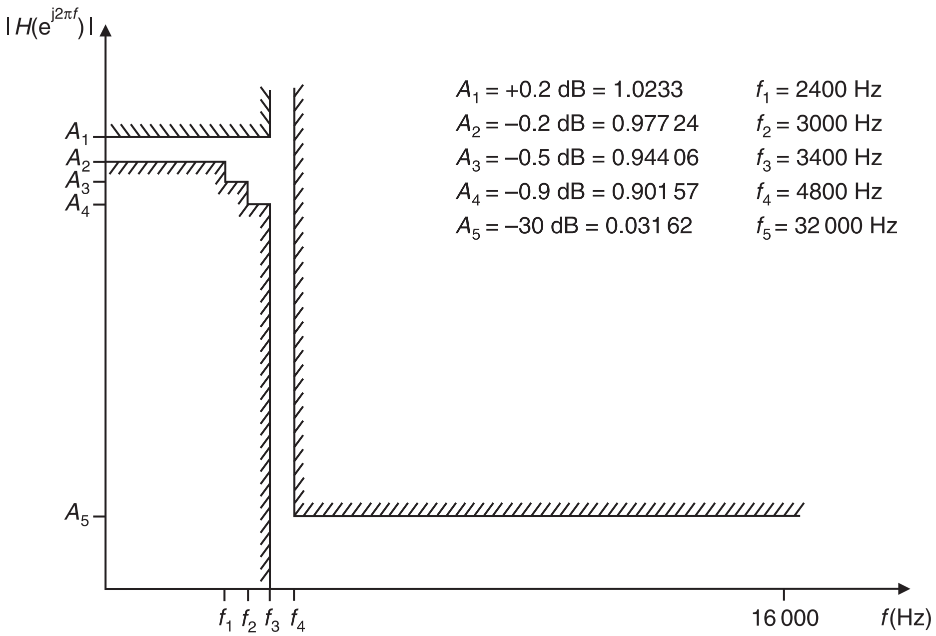

Figure 18: Lowpass PCM filter specifications.

Example 5.7 - Solution

- Two approaches were employed:
  - In the first approach, we simplify the specifications and consider a single passband with constant weight and ideal magnitude response. In this case, the specifications employed correspond to the following description:

    ```
    f3 = 3400; f4 = 4800; f5 = 32000;
    Ap = 0.4; Ar = 30;
    ```

  - One may estimate the required filter order using the command lines:

    ```
    F = [f3 f4]; A = [1 0];
    delta_p = (10^(0.05*Ap) - 1)/(10^(0.05*Ap) + 1);
    delta_r = 10^(-0.05*Ar);
    ripples = [delta_p delta_r];
    M = firpmord(F,A,ripples,f5);
    ```

    which yields $M = 32$.

Example 5.7 - Solution

- (cont.)
  - Such a value, however, is not able to satisfy the filter requirements forcing one to use $M = 34$. The desired filter can then be designed as:

```
wp = f3*2/f5; wr = f4*2/f5;
F1 = [0 f3 f4 f5/2]*2/f5;
A1 = [1 1 0 0];
W1 = [1 delta_p/delta_r];
h = firpm(M,F1,A1,W1);
```

    which yields the filter coefficients provided in Table 13 for $0 \leq n \leq 17$, with $h(n) = h(34 - n)$, and the magnitude response shown in Figure 19.

Example 5.7 - Solution

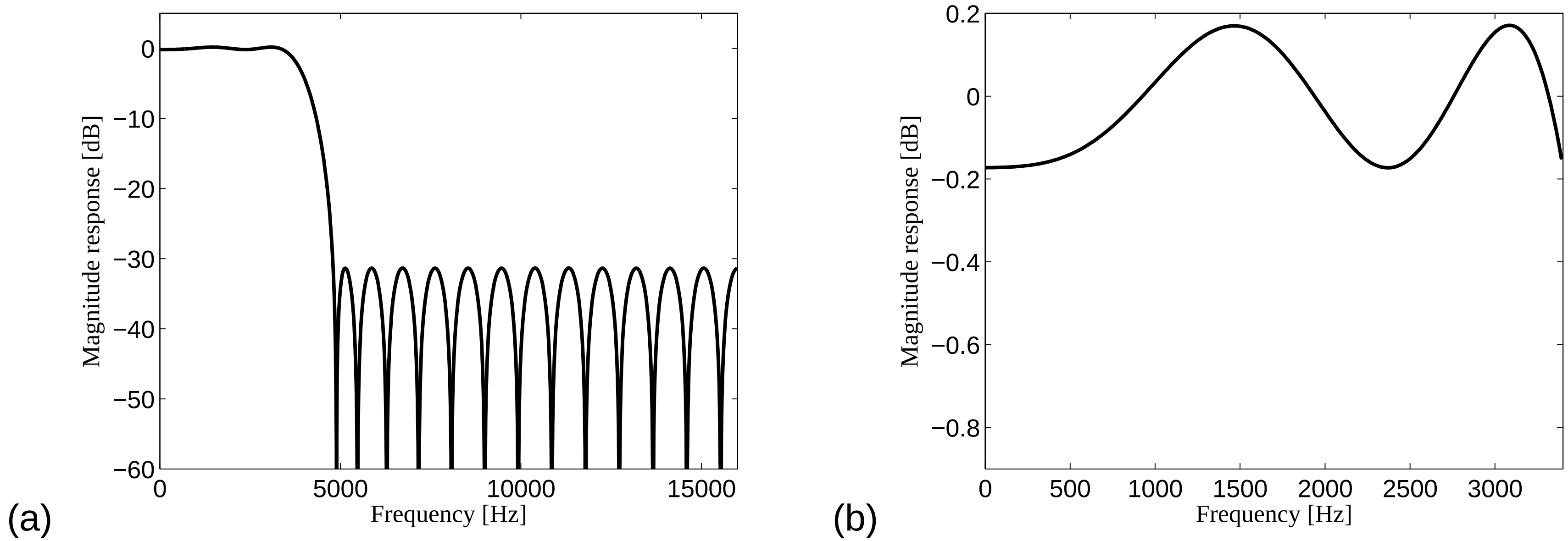

Figure 19: Approach 1: (a) magnitude response; (b) passband detail.

Example 5.7 - Solution

Table 13: Optimal PCM filter obtained with approach 1.

$h(0)$ to $h(17)$			
$h(0) = 0.0153$	$h(5) = -0.0062$	$h(10) = -0.0237$	$h(15) = 0.1569$
$h(1) = 0.0006$	$h(6) = 0.0093$	$h(11) = -0.0482$	$h(16) = 0.2294$
$h(2) = -0.0066$	$h(7) = 0.0226$	$h(12) = -0.0474$	$h(17) = 0.2572$
$h(3) = -0.0139$	$h(8) = 0.0231$	$h(13) = -0.0078$	
$h(4) = -0.0149$	$h(9) = 0.0057$	$h(14) = 0.0674$	

Example 5.7 - Solution

- (cont.)
  - In a second approach, we explore the loosened specifications along the passband and characterize an additional band for the `firpm` command:

```
f1 = 2400; f2 = 3000;
F2 = [0 f1 f2 f3 f4 f5/2]*2/f5;
a1 = 10^(0.05*0.2);
a4 = 10^(0.05*(-0.9));
gain = (a1+a4)/2-0.005;
A2 = [1 1 gain gain 0 0];
delta_p2 = (a1-a4)/2;
W2 = [1 delta_p/delta_p2 delta_p/delta_r];
h2 = firpm(M,F2,A2,W2);
```

Example 5.7 - Solution

- (cont.)
  - In this case, the simplest filter obtained was of order $M = 28$. The filter magnitude response is shown in Figure 20, and its coefficients are listed in Table 14, where only half of the coefficients are shown due to filter symmetry. The remaining coefficients are determined by $h(n) = h(28 - n)$.

Example 5.7 - Solution

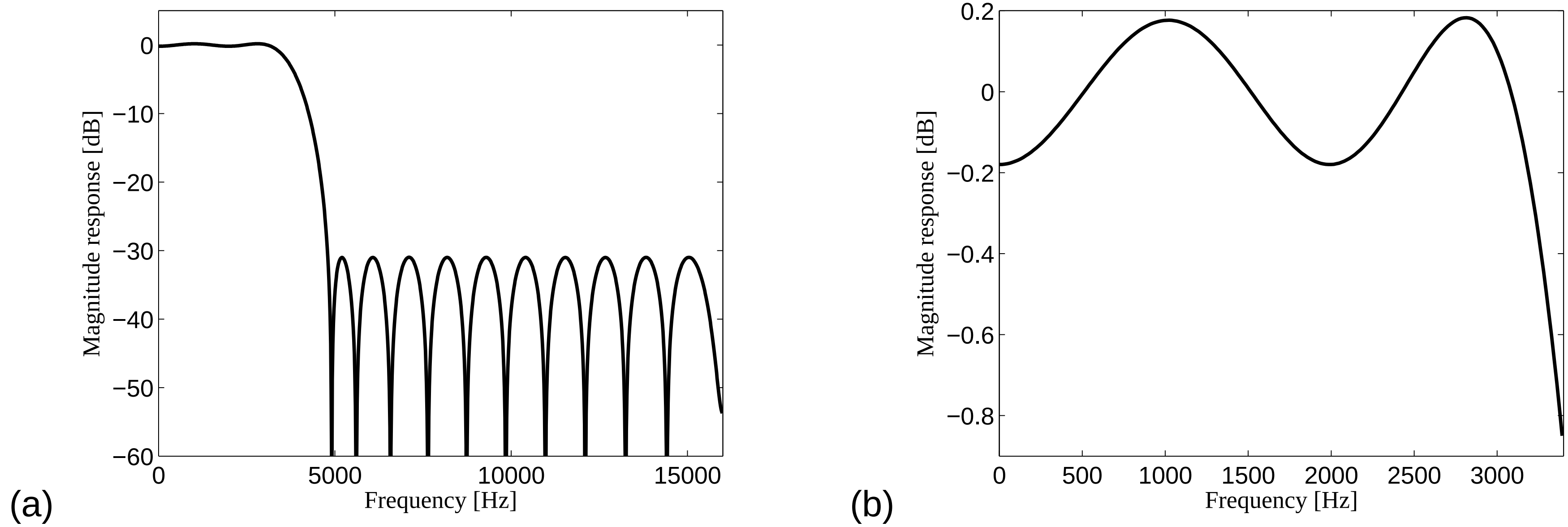

Figure 20: Approach 2: (a) magnitude response; (b) passband detail.

Example 5.7 - Solution

Table 14: Optimal PCM filter obtained with approach 2.

$h(0)$ to $h(14)$			
$h(0) = -0.0186$	$h(4) = 0.0230$	$h(8) = -0.0456$	$h(12) = 0.1579$
$h(1) = -0.0099$	$h(5) = 0.0178$	$h(9) = -0.0426$	$h(13) = 0.2239$
$h(2) = 0.0010$	$h(6) = 0.0017$	$h(10) = 0.0002$	$h(14) = 0.2517$
$h(3) = 0.0114$	$h(7) = -0.0274$	$h(11) = 0.0712$	

WLS–Chebyshev method

- In the standard literature, the design of FIR filters is dominated by the Chebyshev and the weighted-least-squares (WLS) approaches.
- Some applications that use narrowband filters, like frequency-division multiplexing for communications, do require both the minimum stopband attenuation and the total stopband energy to be considered simultaneously.
- For these cases, it can be shown that both the Chebyshev and WLS approaches are unsuitable as they completely disregard one of these two measurements in their objective function.
- A solution to this problem is to combine the positive aspects of the WLS and Chebyshev methods to obtain a design procedure with good characteristics with respect to both the minimum attenuation and the total energy in the stopband.

WLS–Chebyshev method

- Lawson derived a scheme that performs Chebyshev approximation as a limit of a special sequence of weighted-least-p (L_p) approximations, with p fixed. The particular case with $p = 2$ thus relates the Chebyshev approximation to the WLS method.

- The L_2 Lawson algorithm is implemented by a series of WLS approximations using a varying weight matrix $\mathbf{W}_k$, the elements of which are calculated by

$$W_{k+1}^2(\omega) = W_k^2(\omega) B_k(\omega) \tag{162}$$

where

$$B_k(\omega) = |E_k(\omega)| \tag{163}$$

WLS–Chebyshev method

- Convergence of the Lawson algorithm is slow, in practice usually 10 to 15 WLS iterations are required to approximate the Chebyshev solution.
- An efficiently accelerated version of the Lawson algorithm was devised by Lim-Lee-Chen-Yang (LLCY) whose approach is characterized by the weight matrix $\mathbf{W}_k$ recurrently updated by

$$W_{k+1}^2(\omega) = W_k^2(\omega)B_k^e(\omega) \tag{164}$$

where $B_k^e(\omega)$ is the envelope function of $B_k(\omega)$ composed by a set of piecewise linear segments that start and end at consecutive extremes of $B_k(\omega)$.

WLS–Chebyshev method

- Band edges are considered extreme frequencies, and edges from different bands are not connected. In that manner, labeling the extreme frequencies at a particular iteration k as ω_J^*, for $J \in \mathbb{N}$, the envelope function is formed as

$$B_k^e(\omega) = \frac{(\omega - \omega_J^*)B_k(\omega_{J+1}^*) + (\omega_{J+1}^* - \omega)B_k(\omega_J^*)}{(\omega_{J+1}^* - \omega_J^*)}; \ \omega_J^* \leq \omega \leq \omega_{J+1}^* \quad (165)$$

- Figure 21 depicts a typical format of the absolute value of the error function (dash-dotted curve), at any particular iteration, used by the Lawson algorithm to update the weighting function, and its corresponding envelope (solid curve) used by the LLCY algorithm.

WLS–Chebyshev method

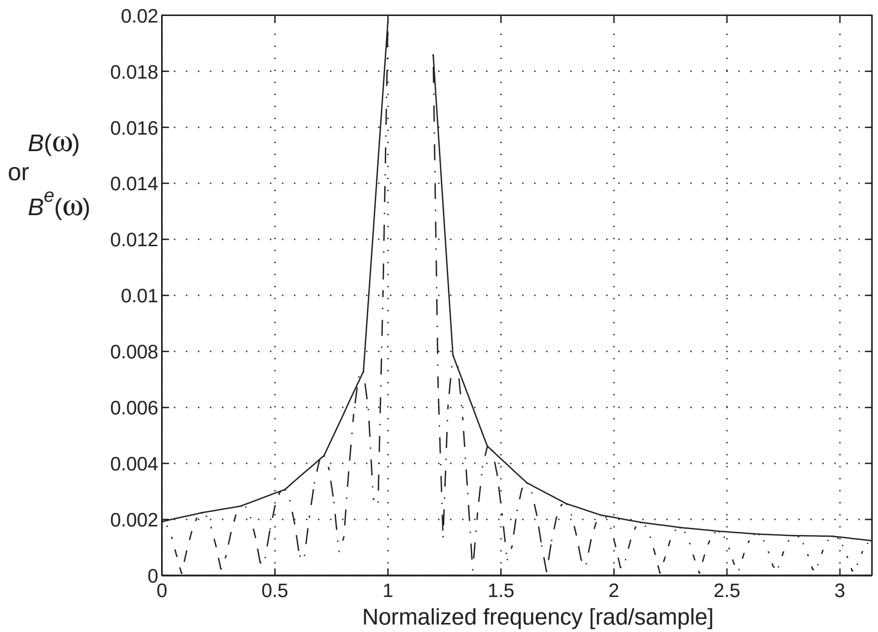

Figure 21: Typical absolute error function $B(\omega)$ (dash-dotted line) and corresponding envelope $B^e(\omega)$ (solid curve).

WLS–Chebyshev method

- Comparing the adjustments used by the Lawson and LLCY algorithms, described in equations (162)–(165), and seen in Figure 21, with the piecewise-constant weight function used by the WLS method, one can devise a very simple approach for designing digital filters that compromises the minimax and WLS constraints.

- The approach consists of a modification of the weight-function updating procedure so that it becomes constant after a particular extreme of the stopband of $B_k(\omega)$, that is,

$$W_{k+1}^2(\omega) = W_k^2(\omega)\beta_k(\omega) \tag{166}$$

WLS–Chebyshev method

- Where, for the modified-Lawson algorithm, $\beta_k(\omega)$ is defined as

$$\beta_k(\omega) \equiv \tilde{B}_k(\omega) = \begin{cases} B_k(\omega), & 0 \leq \omega \leq \omega_J^* \\ B_k(\omega_J^*), & \omega_J^* < \omega \leq \pi \end{cases} \tag{167}$$

and for the modified-LLCY algorithm, $\beta_k(\omega)$ is given by

$$\beta_k(\omega) \equiv \tilde{B}_k^e(\omega) = \begin{cases} B_k^e(\omega), & \text{for } 0 \leq \omega \leq \omega_J^* \\ B_k^e(\omega_J^*), & \text{for } \omega_J^* < \omega \leq \pi \end{cases} \tag{168}$$

where ω_J^* is the Jth extreme value of the stopband of $B(\omega) = |E(\omega)|$.

- The passband values of $B(\omega)$ and $B^e(\omega)$ are left unchanged in equations (167) and (168) to preserve the equiripple property of the minimax method.

WLS–Chebyshev method

- The parameter J is the single design parameter for the WLS-Chebyshev scheme. Choosing $J = 1$, makes the new scheme similar to an equiripple-passband WLS design. On the other hand, choosing J as large as possible, that is, making $\omega_J^* = \pi$, turns the design method into the Lawson or the LLCY schemes.

- An example of the new approach being applied to the generic functions seen in Figure 21 is depicted in Figure 22, where ω_J^* was chosen as the fifth extreme in the filter stopband.

WLS–Chebyshev method

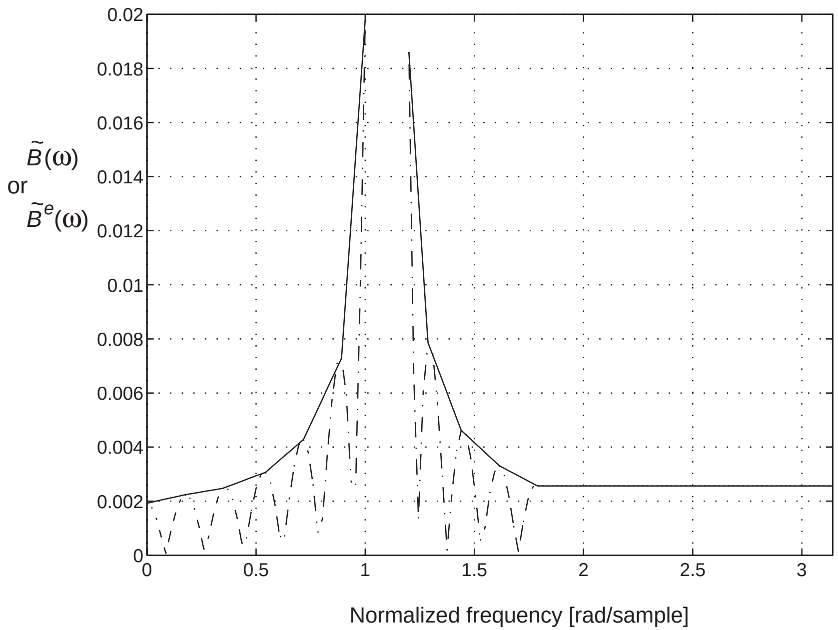

Figure 22: WLS-Chebyshev approach applied to the functions in Figure 21. Modified-Lawson algorithm $\tilde{B}(\omega)$ (dash-dotted curve) and modified-LLCY algorithm $\tilde{B}^e(\omega)$ (solid curve). The curves coincide for $\omega \geq \omega_5^*$.

WLS–Chebyshev method

- The computational complexity of WLS-based algorithms, like the algorithms described here, is of the order of N^3, where N is the length of the filter. This burden, however, can be greatly reduced by taking advantage of the Toeplitz-plus-Hankel internal structure of the matrix $(\mathbf{U}^{\mathrm{T}}\mathbf{W}^2\mathbf{U})$ and by using an efficient grid scheme to minimize the number of frequency values.

- These simplifications make the computational complexity of WLS-based algorithms comparable to that for the minimax approach. The WLS-based methods, however, do have the additional advantage of being easily coded into computer routines.

WLS–Chebyshev method

- The overall implementation of the WLS-Chebyshev algorithm is as follows:
  - (i) Estimate the order M, select $8 \leq K \leq 16$, the maximum number of iterations k_{max}, the value of J, and some small error tolerance $\epsilon > 0$.
  - (ii) Create a frequency grid of KM points within $[0, \pi]$. For linear-phase filters, points in the transition band should be discarded and the remaining points redistributed in the interval $\omega \in [0, \omega_p] \cup [\omega_r, \pi]$.
  - (iii) Set $k = 0$ and form $\mathbf{W}_q$, $\mathbf{d}_q$, and $\mathbf{U}$, as defined in equations (132)–(134), based on Table 12.
  - (iv) Set $k = k + 1$, and determine $\mathbf{p}^*(k)$ from equation (142).
  - (v) Determine the error vector $\mathbf{e}(k)$ as given in equation (130), always using $\mathbf{W}_q$ corresponding to $k = 0$.

WLS–Chebyshev method

- (cont.)
  - (vi) Check if $k > k_{\text{max}}$ or if convergence has been achieved via, for instance, the criterion $| \parallel \mathbf{e}(k) \parallel - \parallel \mathbf{e}(k-1) \parallel | \leq \epsilon$. If so, then go to step (x).
  - (vii) Compute $\{\mathbf{B}_k\}_j = |\{\mathbf{e}(k)\}_j|$, for $j = 0, 1, \ldots, KM$, and $\mathbf{B}_k^e$ as the envelope of $\mathbf{B}_k$.
  - (viii) Find the Jth stopband extreme of $\mathbf{B}_k^e$. For a lowpass filter, consider the interval $\omega \in [\omega_r, \pi]$, starting at ω_r. For a highpass filter, search in the interval $\omega \in [0, \omega_r]$, starting at ω_r. For bandpass filters, consider the intervals $\omega \in [0, \omega_{r_1}]$, starting at ω_{r_1}, and $\omega \in [\omega_{r_2}, \pi]$, starting at ω_{r_2}. For the bandstop filter, look for the extreme in the interval $\omega \in [\omega_{r_1}, \omega_{r_2}]$, starting at both ω_{r_1} and ω_{r_2}.

WLS–Chebyshev method

- (cont.)
  - (ix) Update $\mathbf{W}_{q}^{2}$ using either equation (167) or equation (168), and go back to step (iv).
  - (x) Determine the set of coefficients $h(n)$ of the linear-phase filter, and verify that the specifications are satisfied. If so, then decrease the filter order M and repeat the above procedure starting from step (ii). The best filter would be the one obtained at the iteration just before the specifications are not met. If the specifications are not satisfied at the first attempt, then increase the value of M and repeat the above procedure once again starting at step (ii). In this case, the best filter would be the one obtained when the specifications are first met.

Example 5.8

- Design a bandpass filter satisfying the specification below using the WLS and Chebyshev methods and discuss the results obtained when using the WLS-Chebyshev approach:

$$\left.\begin{aligned} M &= 40 \\ A_p &= 1.0 \text{ dB} \\ \Omega_{r_1} &= \frac{\pi}{2} - 0.4 \text{ rad/s} \\ \Omega_{p_1} &= \frac{\pi}{2} - 0.1 \text{ rad/s} \\ \Omega_{p_2} &= \frac{\pi}{2} + 0.1 \text{ rad/s} \\ \Omega_{r_2} &= \frac{\pi}{2} + 0.4 \text{ rad/s} \\ \Omega_s &= 2\pi \text{ rad/s} \end{aligned}\right\} \tag{169}$$

Example 5.8 - Solution

- As detailed in Example 5.7, the Chebyshev filter can be designed using the `firpm` command:

```
Omega_r1 = pi/2 - 0.4; Omega_p1 = pi/2 - 0.1;
Omega_p2 = pi/2 + 0.1; Omega_r2 = pi/2 + 0.4;
wr1 = Omega_r1/pi; wp1 = Omega_p1/pi;
wp2 = Omega_p2/pi; wr2 = Omega_r2/pi;
Ap = 1; Ar = 40;
delta_p = (10^(0.05*2*Ap) - 1)/(10^(0.05*2*Ap) + 1);
delta_r = 10^(-0.05*Ar);
F1 = [0 wr1 wp1 wp2 wr2 1];
A1 = [0 0 1 1 0 0];
W1 = [delta_p/delta_r 1 delta_p/delta_r];
h_cheb = firpm(M,F1,A1,W1);
```

Example 5.8 - Solution

- The WLS filter is designed using `firls` command whose syntax is entirely analogous to the `firpm` command:

```
h_wls = firls(M,F1,A1,W1);
```

- The magnitude responses for the Chebyshev and WLS filters designed as above are seen in Figure 23, subplots (a) and (d), which correspond to the $J = 10$ and $J = 1$ cases, respectively.

- Other values of J, whose magnitude responses are also shown in Figure 23, require a specific MATLAB script implementing the WLS-Chebyshev approach, as detailed earlier in this subsection.

Example 5.8 - Solution

- Table 15 shows half of the filter coefficients for the case when $J = 3$. The remaining coefficients are obtained as $h(n) = h(40 - n)$.
- Figure 24 shows the tradeoff between the stopband minimum attenuation and total stopband energy when J varies from 1 to 10.
- Notice how the two extremes correspond to optimal values for the attenuation and energy figures of merit, respectively. On the other hand, the same extremes are also the worst case scenarios for the energy and the attenuation in the stopband. In this example, a good compromise between the two measures can be obtained when $J = 3$.

Example 5.8 - Solution

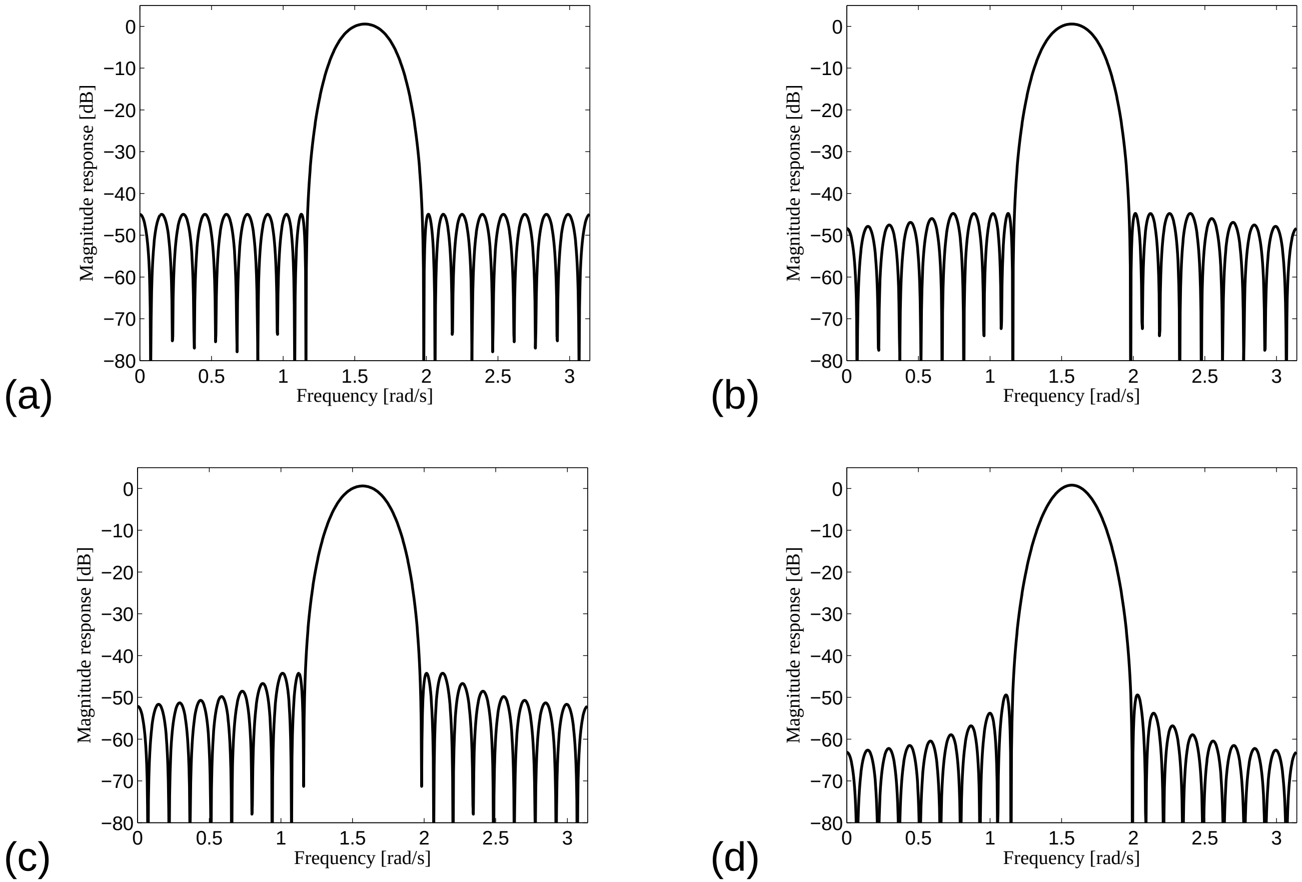

Figure 23: Magnitude responses using WLS-Chebyshev method with: (a) $J = 10$; (b) $J = 5$; (c) $J = 3$; (d) $J = 1$.

Example 5.8 - Solution

Table 15: Coefficients of the bandpass filter designed with the WLS-Chebyshev method with $J = 3$.

$h(0)$ to $h(20)$			
$h(0) = -0.0035$	$h(6) = -0.0052$	$h(12) = 0.0653$	$h(18) = -0.1349$
$h(1) = -0.0000$	$h(7) = -0.0000$	$h(13) = 0.0000$	$h(19) = -0.0000$
$h(2) = 0.0043$	$h(8) = 0.0190$	$h(14) = -0.0929$	$h(20) = 0.1410$
$h(3) = 0.0000$	$h(9) = 0.0000$	$h(15) = -0.0000$	
$h(4) = -0.0020$	$h(10) = -0.0396$	$h(16) = 0.1176$	
$h(5) = 0.0000$	$h(11) = -0.0000$	$h(17) = 0.0000$	

Example 5.8 - Solution

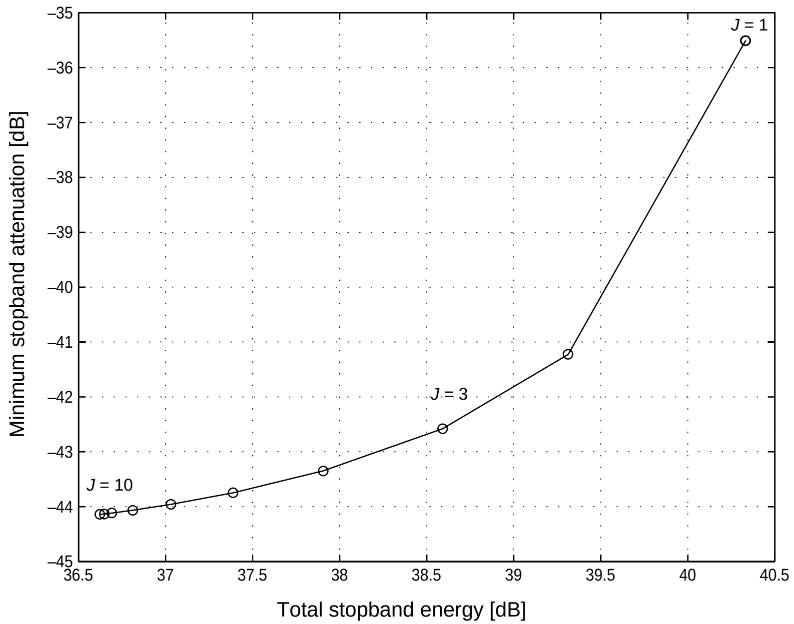

Figure 24: Tradeoff between the minimum stopband attenuation and total stopband energy using the WLS-Chebyshev method.

Do-it-yourself: FIR filter approximations

- **Experiment 5.1:** The output signal of a differentiator device to a complex sinusoid input is given by

$$y(t) = \frac{dx(t)}{dt} = \frac{de^{j\Omega t}}{dt} = j\Omega e^{j\Omega t} \tag{170}$$

- Hence, the ideal differentiator has a magnitude gain proportional to the input frequency Ω and a phase shift of $\pm\frac{\pi}{2}$ depending on the sign of Ω.

- For discrete-time systems, this analysis holds for the digital frequency within $\omega \in [-\frac{F_s}{2}, \frac{F_s}{2}]$, as depicted in Figure 2.

Do-it-yourself: FIR filter approximations

- Consider 1-second interval of a cosine signal generated in MATLAB as

  ```
  Fs = 1500; Ts = 1/Fs; t = 0:Ts:1-Ts;
  fc = 200;
  x = cos(2*pi*fc.*t);
  ```

  whose output to a differentiator is

  ```
  y1 = -2*pi*fc*sin(2*pi*fc.*t);
  ```

  as discussed above.

- The differentiation operation can be approximated by

$$y_2(t) \approx \frac{x(t+\Delta t) - x(t)}{\Delta t} \tag{171}$$

  leading, in the discrete-time domain, to the output

$$y_2(n) \approx \frac{\cos(2\pi f_c (n+1) T_s) - \cos(2\pi f_c n T_s)}{T_s} \tag{172}$$

Do-it-yourself: FIR filter approximations

- This approximation can be determined in MATLAB as

```
y2 = [0 diff(x)]/Ts;
```

  which, in the z domain, corresponds to the transfer function

$$H_2(z) = \frac{(z-1)}{T_s} \tag{173}$$

  whose magnitude response is shown as the dashed line in Figure 25a.

- In this plot, one can notice that this first-order approximation works very well for small values of f_c, but deviates from the desired response (indicated by the solid line) as f_c approximates $\frac{F_s}{2}$. This fact motivates one to design better differentiators.

Do-it-yourself: FIR filter approximations

- Using a rectangular window, the impulse response of a differentiator device is obtained directly from Table 1, and can be determined in MATLAB, for an odd length N, as

```
N = 45;
h3 = zeros(N,1);
for n = -(N-1)/2:(N-1)/2,
   if n ~= 0,
      h3((N+1)/2+n) = ((-1)^n)/n;
   end;
end;
```

  yielding the frequency response

```
[H3,W] = freqz(h3,1);
```

Do-it-yourself: FIR filter approximations

- Using any other window function, as for instance the Blackman window, one may get

```
h4 = h3.*blackman(N);
H4 = freqz(h4,1);
```

- A differentiator may also be designed with Chebyshev algorithm using `firpm` command.

- In this case, one must specify vectors `F = [0 f1 f2 1]` and `A = [0 pi*f1 pi*f2 0]`, characterizing the desired response, which should vary from 0 to π`f1` within the differentiator passband $[0,$ `f1`$]$ and from π`f2` to 0 within the normalized interval $[$`f2`$, 1]$.

Do-it-yourself: FIR filter approximations

- An example of such a design is given by

```
F = [0 0.9 0.91 1];
A = [0 0.9*pi 0.91*pi 0];
h5 = firpm(N-1,F,A,'differentiator');
H5 = freqz(h5,1);
```

- The magnitude responses of all differentiators designed above are shown in Figure 25b.

Do-it-yourself: FIR filter approximations

(a) 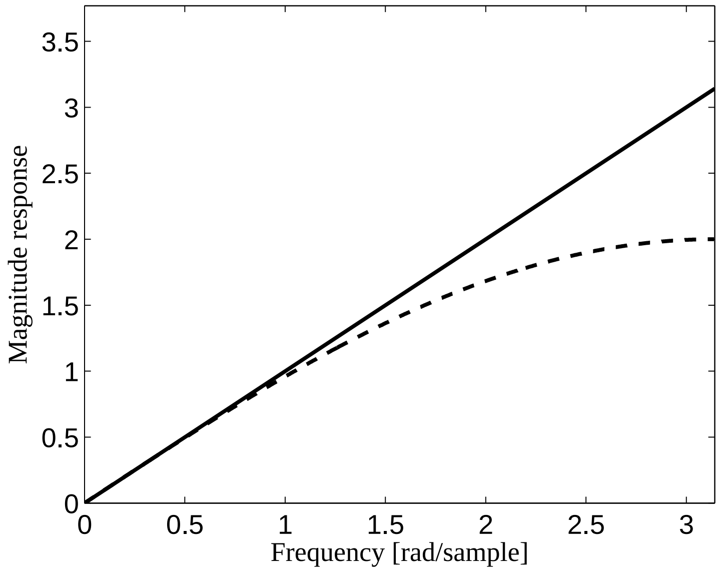

(b) 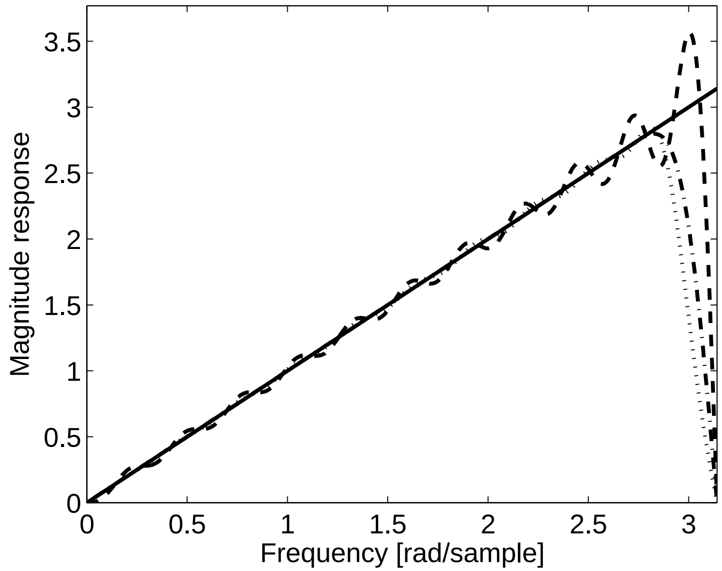

Figure 25: Magnitude responses of differentiators in Experiment 5.1: (a) ideal (solid line) and first-order approximation (dashed line); (b) ideal (solid line), rectangular window (dashed line), Blackman window (dash-dotted line), and Chebyshev algorithm (dotted line).

Do-it-yourself: FIR filter approximations

- **Experiment 5.2:** Using the specifications

$$\left.\begin{aligned} N &= 20 \\ \omega_p &= 0.1 \\ \omega_r &= 0.2 \\ \omega_s &= 2 \end{aligned}\right\} \qquad (174)$$

a nice lowpass FIR filter can be designed with, for instance, the MATLAB command `firpm` as given by

```
N = 20; Freq = [0 0.1 0.2 1]; Weight = [1 1 0 0];
h = firpm(N,Freq,Weight);
```

- The magnitude response of the corresponding filter is depicted in Figure 26, along with the one of the moving average filter with $N = 20$ employed in Experiments 1.3 and 2.2.

Do-it-yourself: FIR filter approximations

- From this figure, one clearly notices how the `firpm` filter can sustain a flatter passband as desired, better preserving the two sinusoidal components in signal `x` from Experiment 1.3, while strongly attenuating the noise components within the specified stopband, as seen in Figure 27.

Do-it-yourself: FIR filter approximations

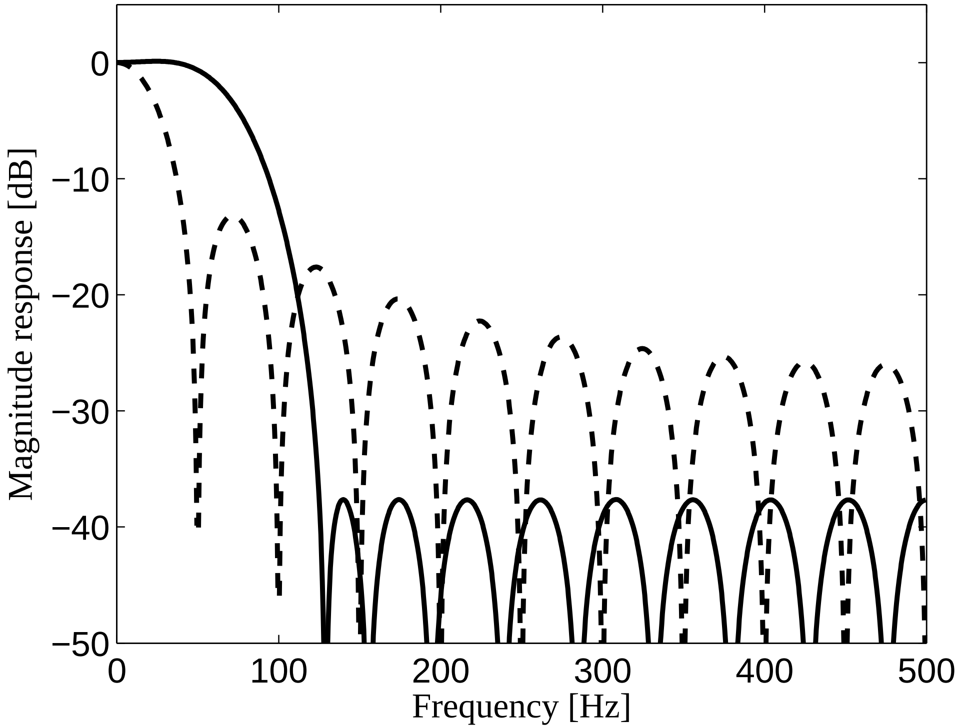

Figure 26: Magnitude responses of lowpass filter with $N = 20$ in Experiment 5.2: `firpm` (solid line) and moving-average (dashed line).

Do-it-yourself: FIR filter approximations

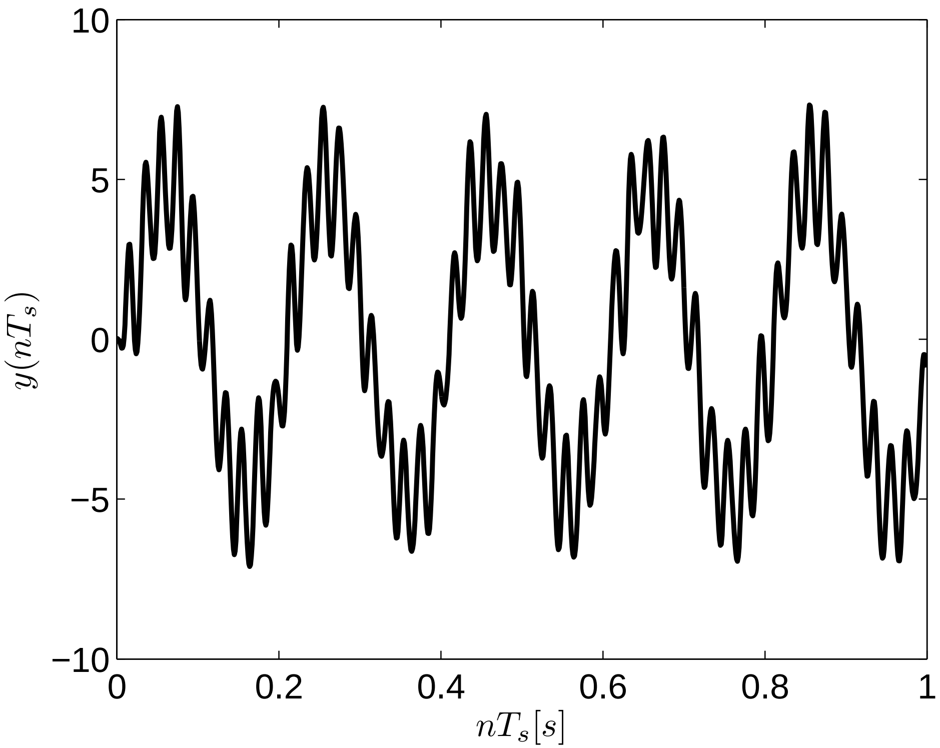

Figure 27: Output signal from `firpm` filter in Experiment 5.2 for noisy sinusoidal components in `x` signal in Experiment 1.3.